DEUQUA Spec. Pub., 1, 53–77, 2018
https://doi.org/10.5194/deuquasp-1-53-2018

Open Access DEUQUA Special Publications

Field Trip D (27 September 2018): characteristics and development of the Mesozoic–Tertiary weathering mantle and Pleistocene periglacial slope deposits in the Hintertaunus mountainous region

Peter Felix-Henningsen

Institut f. Bodenkunde und Bodenerhaltung, Justus-Liebig-Universität Gießen, Heinrich-Buff-Ring 26, 35392 Gießen, Germany

Correspondence: Peter Felix-Henningsen (peter.felix-h@umwelt.uni-giessen.de)

Relevant dates: Published: 20 August 2018

How to cite: Felix-Henningsen, P.: Field Trip D (27 September 2018): characteristics and development of the Mesozoic–Tertiary weathering mantle and Pleistocene periglacial slope deposits in the Hintertaunus mountainous region, DEUQUA Spec. Pub., 1, 53–77, https://doi.org/10.5194/deuquasp-1-53-2018, 2018.

Abstract: The Devonian slates and sandstones of the Rhenish Massif were subject to deep and intensive weathering under (sub)tropical climate conditions during the Cretaceous, the Paleogene and the Neogene, which caused the development of a weathering mantle (regolith) > 100 m thick, consisting of kaolinitic saprolite and paleosols as well as correlated sediments. Especially the tectonic uplift of the Rhenish Massif and climate change during the Neogene and the Pleistocene led to a vast denudation of the weathering mantle. Only in less uplifted areas of the mountainous region did thick remnants of saprolites remain, and they were covered by Neogene sediments as well as Quaternary periglacial slope deposits. As the kaolinitic weathering products serve as raw materials for the clay industry, unique exposures are available in the Hintertaunus which offer impressive insights into the landscape development of the past ~ 80 million years: the excursion proceeds from Giessen to Limburg and further south and southwest to the eastern and western Hintertaunus area. At site 1 near the village of Langhecke, characteristics and properties of the fresh, unweathered slates will be demonstrated. Excursion sites 2 and 3 are situated near the village of Eisenbach. In two open-cast clay mines, both a terrestrial and a semi-terrestrial saprolite from silt slate, covered by periglacial layers, are exposed. Properties and genesis will be discussed on the basis of morphological characteristics and mineralogical and geochemical analyses, as well as isovolumetric elemental mass balances. At site 4 a former basalt quarry near the village of Biebrich exposes a Paleogene Plinthosol above saprolite. The autochthonous paleosol was preserved below Upper Oligocene basalt tuff and periglacial layers. Site 5 is situated within a huge pit for mining of Upper Oligocene to Miocene quartz gravel near the village of Wasenbach. A Miocene Plinthosol developed from alluvial sediments on top of the gravel beds and was covered by periglacial slope deposits. At nearly all sites the basal layers of the periglacial cover beds consist of kaolinitic paleosol/saprolite material, which has an important influence on the site properties of the Holocene soils.

Kurzfassung:

Unter (sub-)tropischen Klimabedingungen während der Kreidezeit, sowie im Paläogen und Neogen, waren die devonischen Schiefer und Sandsteine einer intensiven Verwitterung ausgesetzt durch die eine > 100 m mächtige Verwitterungsdecke (Regolith) aus kaolinitischen Saprolitzonen, Paläoböden und korrelaten Sedimenten entstand. Tektonische Hebung des Rheinischen Schiefergebirges und Klimawechsel im Neogen und Pleistozän führten dazu, dass die Verwitterungsdecke in weiten Bereich wieder abgetragen wurde. Nur in den schwächer gehobenen Gebieten des Mittelgebirges, wie im Hintertaunus, blieben mächtige Reste der Verwitterungsdecke erhalten, die von neogenen Sedimenten und quartären periglazialen Deckschichten überlagert wurden. Da die kaolinitischen Verwitterungsprodukte wertvolle Rohstoffe für die Tonindustrie darstellen, entstanden im Hintertaunus einzigartige Aufschlüsse, an denen die Landschaftsentwicklung der vergangenen 80 Mio. Jahre eindrucksvoll sichtbar wird:

Die Exkursion führt von Gießen nach Limburg und von dort nach S und SW in den östlichen und westlichen Hintertaunus. Am Exkursionspunkt 1, bei der Ortschaft Langhecke, werden die Merkmale und Eigenschaften der frischen, unverwitterten Schiefer demonstriert. Die Exkursionspunkte 2 und 3 befinden sich nahe der Ortschaft Eisenbach. In zwei Tongruben sind ein terrestrischer und ein semiterrestrischer Saprolit aus Schluffschiefer aufgeschlossen, die von periglaziären Deckschichten überlagert werden. Auf Basis der morphologischen Merkmale, der mineralogischen und geochemischen Analysendaten sowie den Ergebnissen isovolumetrischer Massenbilanzen werden die Eigenschaften und Genese der Verwitterungsdecke und ihre Überprägung im Pleistozän diskutiert. Am Standort 4, nahe der Ortschaft Biebrich, ist in einem ehemaligen Steinbruch ein autochthoner Plinthosol aus dem Paläogen aufgeschlossen, der unter oberoligozänem Basalttuff konserviert und von gegliederten periglaziären Deckschichten überlagert wurde. Exkursionspunkt 5 befindet sich in einem großen Kiesabbau nahe der Ortschaft Wasenbach, in dem oberoligozäne – untermiozäne Quarzschotter und -sande des Vallendar-Flusssystems abgebaut werden. Ein miozäner Plinthosol entstand aus Hochflutsedimenten oberhalb der fluviatilen Kiese und wurde von periglaziären Deckschichten überlagert. Deren Basislage besteht hier, wie an den anderen Standorten, aus dem kaolinitischen Substrat des unterlagernden Saprolits/Paläobodens und hat damit einen bedeutenden Einfluss auf die Standorteigenschaften der holozänen Böden.

1 Introduction

The bedrock areas in mountainous regions of Middle Europe, which was a continent during the Mesozoic and Tertiary, were subject to deep weathering under (sub)tropical humid climate conditions, which caused the formation of a kaolinitic weathering mantle tens to hundreds of metres thick, consisting of a paleosol above saprolite (Fig. 1). Details about distribution and genesis as well as comprehensive references are published in Felix-Henningsen (1990, 1994, 2015).

Due to tectonic uplift of the former planation plains and climate changes during the Neogene and the Quaternary, the Mesozoic–Tertiary weathering mantle (MTV) was in part or completely subject to erosion. Especially the strong uplift during the Quaternary and periglacial conditions during the cold periods strongly supported the removal of the weathering mantle and led to the expansion of a sequence of periglacial layers above the truncated weathering mantle (Felix-Henningsen et al., 1991; Sauer and Felix-Henningsen, 2006, Fig. 2). Only in areas with weaker tectonic uplift did more or less thick remnants of the weathering mantle remain.

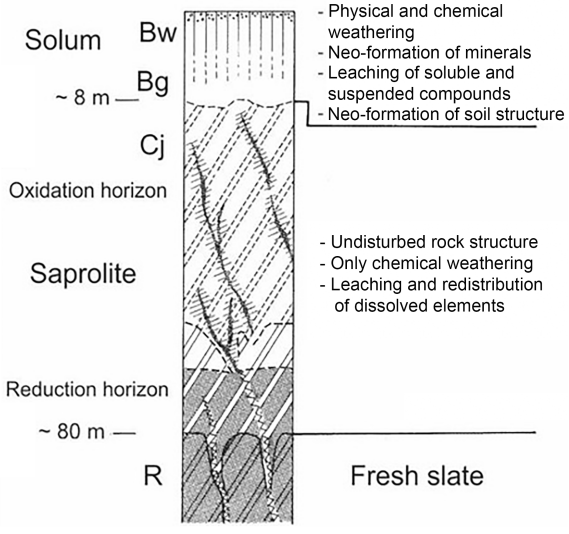

Figure 1. Organization of the complete Mesozoic–Tertiary weathering mantle (MTV) of the Rhenish Massif with the units fresh rock, saprolite and solum.

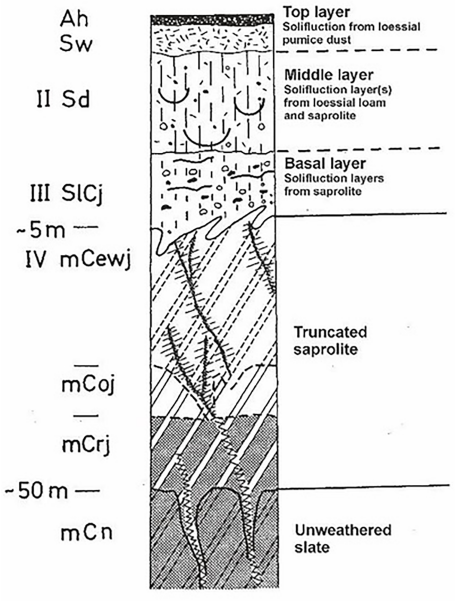

Figure 2. Organization of the more or less denudated Mesozoic–Tertiary weathering mantle (MTV) of the Rhenish Massif on remnants of the planation planes, covered by Pleistocene periglacial layers (top layer is referred to as "main layer" in the text).

Figure 3. Saprolite of the Mesozoic–Tertiary weathering mantle with interfingered transition between the white, bleached oxidation horizon and the black reduction horizon below. The saprolite of both horizons displays a well-preserved rock structure, but it is soft and friable.

Autochthonous kaolinitic paleosols of Cretaceous to Neogene age show characteristics of soils of the modern tropical regions (e.g. Ferralsols, Plinthosols). They developed at the former land surface by processes of soil formation, such as chemical and physical weathering and bioturbation. Remnants of such paleosols occur in small areas, protected against erosion by a cover of Tertiary sediments or volcanic rocks (Fig. 4).

Saprolites developed below the paleosols when the weathering front exceeded the depth of the soil. They are exclu-

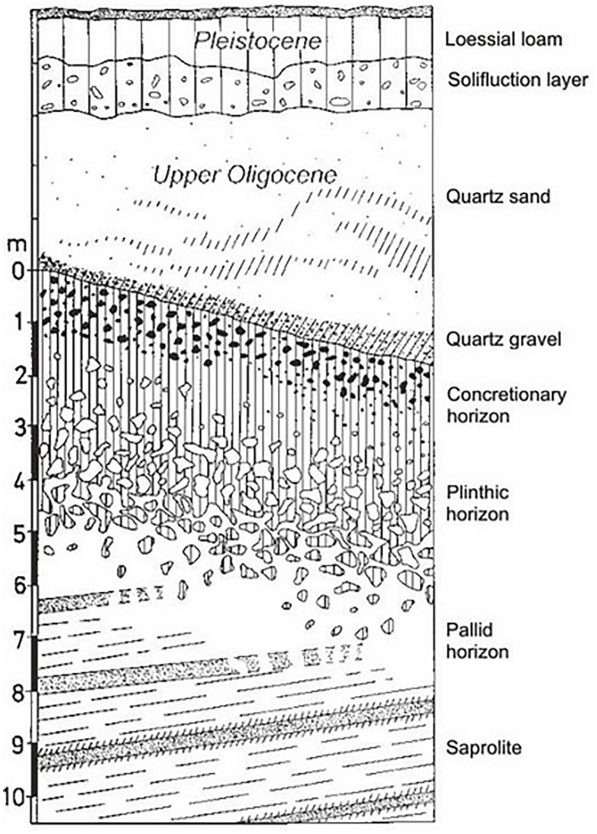

Figure 4. Pre-Upper Oligocene fossil ferrallitic Plinthosol above saprolite from silt slate, covered by Upper Oligocene fluvial sediments and periglacial layers, near Bengen, Rhenish Massif (for details see Felix-Henningsen and Wiechmann, 1985).

sively chemically weathered bedrock and show the preserved rock structure because with increasing depth of the weathering front the physical forces (swelling and shrinkage, rooting, bioturbation, frost pressure) intermitted, while dissolution of minerals and leaching of elements under sufficient precipitation proceeded unhampered (Fig. 1).

The excursion aims to present unique sections of the thick weathering mantle in the Hintertaunus (literal: back of the Taunus) region, which is a part of the eastern Rhenish Massif (Fig. 6), in order to discuss properties and genesis, as well as the Quaternary superimposition and the consequence for the site properties of Holocene soils. Due to a lesser tectonic uplift and weak denudation of the Cretaceous to Paleogene planation areas, more or less thicker remnants of the weathering mantle are well preserved. The excursion presents fresh slates as parent rock as well as unique exposures of terrestrial and semi-terrestrial saprolites and autochthonous paleosols of Paleogene and Miocene age. Furthermore, periglacial superficial layers above saprolite and paleosols, exposed in deep profiles, allow insight into the processes of periglacial overprinting of the MTV. In detail, the following topics will be presented and discussed:

Table 1. Geological development of the Rhenish Massif since the Mesozoic.

Era	Formation	Series	Start (Ma)	Geomorphological processes	Climate
Cenozoic	Quaternary	Holocene	0.01	weathering, erosion, especially of unconsolidated material	moderate humid
		Pleistocene	2.8	East Eifel volcanism, formation of the transverse valley of the Rhine river through the Rhenish Massif, strong tectonical uplift, formation of river terraces and periglacial layers	alternation of cold periglacial periods and moderately warm interglacial periods
	Tertiary	Pliocene	5	weak tectonical uplift, weathering and strong denudation of the old weathering mantle due to climatic change, deposition of quartz gravels at river terraces	change from warm humid to moderate humid, warm arid phases
	Neogene	Miocene	23	volcanism (e.g. Vogelsberg), phase of kaolinitic deep weathering, denudation, sedimentation of kaolinitic clays formation of the recent river system	warm humid, warm arid phases
	Tertiary Paleogene	Oligocene	38	strong tectonic uplift, formation of fault blocks and fault troughs, weathering and denudation, sedimentation of kaolinitic clays western Eifel volcanism, sub-volcanoes of the Siebengebirge	warm humid with moderate and arid phases
		Eocene	55	peneplanation, kaolinitic deep weathering and soil formation, phases of tectonic uplift with denudation of soils and sedimentation of kaolinitic clays.	warm humid, warm arid phases
		Palaeocene	65	peneplanation, kaolinitic deep weathering and soil formation	warm humid
Mesozoic	Cretaceous	Upper Lower	100 145	peneplanation, deep weathering, marine transgressions at the margins of the Rhenish Massif	warm humid

- characteristics, properties and mineralogical composition of Lower Devonian slates as parent rock of the MTV;
- morphological characteristics as well as geochemical and mineralogical properties of different saprolite zones and their genesis;
- characteristics, properties, genesis and classification of autochthonous kaolinitic paleosols of Paleogene and Miocene age;
- organization, stratigraphy and properties of periglacial layers;
- demonstration and discussion of methodological approaches of clay mineral analyses and isovolumetric element mass balances.

2 The excursion area

2.1 Geomorphology of the Hintertaunus region

Table 1 shows the timescale of the geological development of the Rhenish Massif. Of specific interest for the topic of this excursion is the younger geologic history of the past 195 Ma from the Cretaceous to the Holocene. The Taunus forms the tectonically uparched, south-eastern part of the middle mountains, separated by the Lahn syncline from the Westerwald in the north. The Hintertaunus area slants down from the High Taunus (up to 879 m a.s.l.) in a north-eastern direction to the Lahn valley at Limburg (113 m a.s.l.). The crest of the High Taunus consists of massive Taunus quartzite (upper Siegen, lowest Lower Devonian), followed to the north and north-west by Hunsrück slates from marine silt and fine sand. North of the village of Eisenbach at the edge of the Limburg basin the bedrock changes narrowly with clay slate and quartzite of the Upper Ems and calcareous slates, diabase and marine tuffs (Schalstein) of the Middle and Upper Devonian (Felix-Henningsen and Requadt, 1985). In the western Hintertaunus alternating layers of quarzitic Paleogene sandstones, silt slates and marine tuffs represent the Lower Devonian rocks, locally mounted by Eocene to Lower Miocene volcanoes (Müller, 1973).

In a paleo-river system, which existed from the middle Eocene to the Upper Oligocene, fluvial milky quartz gravels (Vallendar gravel) were deposited in valleys and basins, where they reached a thickness of up to several tens of me-

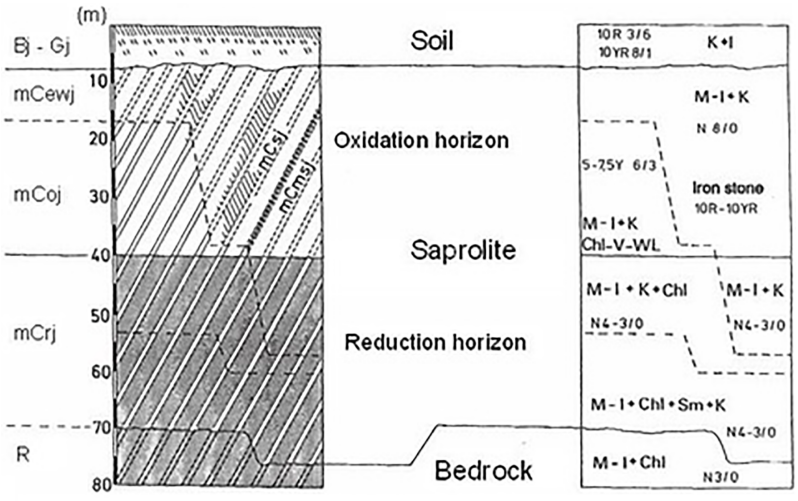

Figure 5. Morphological and mineralogical organization of the Mesozoic–Tertiary weathering mantle (MTV) of the Rhenish Massif. Bj-Gj is terrestrial or semi-terrestrial fersiallitic soil horizons, mCewj is bleached saprolite, mCoj is oxidized saprolite, mCrj is reduced saprolite and R is fresh rock; K is kaolinite, I is illite, M is muscovite, Chl-V-WL is chlorite–vermiculite mixed layer minerals, Sm is smectite and Chl is chlorite.

tres (Ahlburg, 1915; Löhnertz, 1978; Andres et al., 1974; Semmel, 1984). In the western Rhenish Massif the paleo-river course can be traced parallel to the Mosel river down to the tectonical basin of Neuwied (Semmel, 1984). Requadt (1990) concludes that the Vallendar gravels were originally deposited as sediments of a Middle to Upper Oligocene (33–30 Ma) marine transgression advancing from the Mainz basin in the south of the Rhenish Massif towards the north. In this period, a connection existed between the northern alpine Molasse basin through the Upper Rhine fault trough and the Hessian basin to the North Atlantic (Walter, 1995). In a second phase, during tectonic uplift of the area, the eroded material of the weathering mantle was repeatedly redistributed and finally deposited in river valleys. Requadt and Buhr (1989) identified five terraces with deposits of milky quartz gravel in different altitudes adjacent to the lower Lahn valley. The tectonic uplift during the Pliocene favoured the fluvial dissection of the excursion area, which led to erosion of a great part of the Vallendar gravel and the underlying weathering mantle (Andres et al., 1974). Periglacial solifluction during the Upper Pleistocene caused extensive redistribution of the exposed paleosols, saprolites and Vallendar gravel and the formation of the basal layer. On flat slopes and in plain areas, loess, deposited during the glacial and afterwards partly redistributed by solifluction, remained as the middle layer. Area-wide, an upper layer of redistributed loess, mixed with pumice of the Laacher See volcano eruption, was deposited by eolian sedimentation and solifluction during the Younger Dryas period (Felix-Henningsen et al., 1991). Thick loess deposits within the basins of Limburg and Idstein were the parent material of fertile Holocene Luvisols, intensively used by agriculture.

The rivers Aar, Wörsbach and Emsbach (from west to east) are tributaries of the lower Lahn river, which drain the excursion area. The average annual temperatures are 8.5 to 9 °C in lower altitudes and about 7 °C above 500 m a.s.l. Annual precipitation amounts to 650–750 mm.

2.2 The Mesozoic–Tertiary weathering mantle

The bedrock of the Rhenish Massif consists of Devonian slates and sandstones, which are exposed to continental conditions at least since the Jurassic. During this period of about 200 Ma in total, discrete phases, each of Ma duration with (sub)tropical humid (Cretaceous and Paleogene, middle Miocene), semi-arid (Upper Oligocene, Lower Miocene), subtropical to moderate (Neogene) and moderate to arctic climate (Quaternary), influenced the development of the weathering mantle, paleosols and relief forms. In periods of millions of years with a humid (sub)tropical climate during the Upper Cretaceous and Tertiary, a saprolite more than 150 m thick (Spies, 1986) developed below a kaolinitic paleosol (Figs. 1 and 4), when the weathering front advanced with a higher rate to greater depths than the lowering of the land surface by erosion. The progression of the weathering front to greater depths on crystalline rocks shows rates of 1 to 5 cm in 1000 years under recent humid tropical climate conditions (references in Felix-Henningsen, 2015). Therefore, saprolites testify to periods lasting millions of years with warm humid climatic conditions, high weathering intensity and an extremely stable land surface due to a dense vegetation cover.

The occurrence of the MTV is bound to planation plains, which developed by extensive denudation during the Cretaceous until the Paleogene. Their remnants are preserved in weaker uplifted areas of the Rhenish Massif, mainly at the

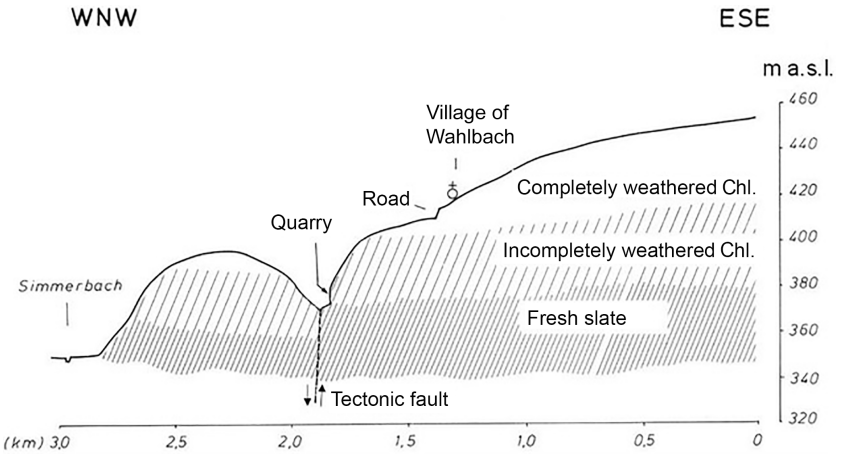

Figure 6. Simple classification of the weathering intensity of saprolite from Devonian slates of the Rhenish Massif (used for mapping and geomorphological investigations; example is from the dissected planation plane of the Hunsrück area): an upper zone, in which chlorites are completely weathered to kaolinite, and a lower zone, with incomplete kaolinitization of chlorite.

edges and within tectonic basins of the mountainous region. Also in the flat upland area of the Hintertaunus, which during the Neogene was already affected by tectonic subsidence, leading over to the downthrown fault blocks of the basins of Idstein, Limburg and the Westerwald, thick sections of the saprolite remained.

Saprolites from Lower Devonian slates are characterized by their preserved rock structure, a lower mechanical stability than the fresh slates and a change of colour due to weathering of silicates and oxidation. Morphological characteristics as well as chemical and mineralogical properties of saprolites, which in a similar way are distributed in weathering mantles of the recent tropics, change with depth, because the age and intensity of weathering decrease from the basis of the paleosol towards the weathering front at the basis of the saprolite. Thus, a vertical sequence of upper, middle and lower saprolite zones can be defined by their morphological characteristics as well as mineralogical, geochemical and physical properties (Felix-Henningsen, 1994, Fig. 5). Due to weathering of silicates and leaching of the dissolved ions, which do not contribute to the neo-formation of clay minerals, the bulk density (volume weight, vol-wt) and mechanical stability decrease from the weathering front towards the surface as a consequence of increasing mass loss (Table 2), porosity and permeability. In the lowest saprolite zone the primary Fe–Mg chlorites, which are the minerals with the lowest stability, changed to smectite under reducing conditions and chlorite–vermiculite mixed layer (m.l.) minerals under oxidizing conditions as intermediate products. With increasing intensity of weathering and leaching in the upper saprolite zones, these secondary minerals were dissolved and kaolinites precipitated (Fig. 5), while bases and silica were leached (e.g. Tables 3–7). For mapping of the weathering mantle and identification of tectonic faults, a subdivision of the saprolite in two mineralogical zones is useful (Spies, 1986): an upper zone with complete transformation of chlorite into kaolinite and a lower zone with incomplete transformation (Fig. 6).

Table 2. Bulk densities (b.d.) and Ti / Zr ratios of fresh slate and saprolite zones (Eisenbach Töpferkaute). Absolute bulk mass losses (b.m.l. in $g\,cm^{-3}$) = b.d. Cn − b.d. R; relative bulk mass losses (b.m.l. in %) = (b.m.l. Cj / b.m.l. R) · 100; Ti / Zr = Ti (mass %) × 10^3 / Zr ($mg\,kg^{-1}$).

Horizon	Depth (m)	b.d. ($g\,cm^{-3}$)	b.m.l. ($g\,cm^{-3}$)	b.m.l. (%)	Ti / Zr ($mg\,kg^{-1}$)
Cj1	2–15	1.70	0.88	−34	5.21
Cj4	20–24	1.85	0.73	−28	2.35
Cj5	24–30	2.25	0.33	−13	4.38
R	> 30	2.58	0	0	4.39

The mass loss of Al indicates that chlorite was not quantitatively transformed into kaolinite. Acid conditions in the weathering zone and presumably high contents of dissolved organic carbon in the pore solution, which derived from the decomposition of organic matter in the soil, supported the solubility and leaching of Al ions.

The morphological and geochemical characteristics of saprolites also depend on Cretaceous and Paleogene relief conditions. Red- or brown-coloured terrestrial saprolites, with high contents of pedogenic Fe and Mn oxides, weathered under oxidizing conditions and the influence of percolating water. In lower areas of the undulating planation surface, a high groundwater table caused the formation of semiterrestrial saprolites. As a consequence of weathering under groundwater saturation and leaching of dissolved metal ions under reducing conditions, these saprolites display a white colour due to bleaching (Felix-Henningsen, 1994).

Figure 7. Hintertaunus, south-eastern Rhenish Massif, with locations of the excursion sites.

The known autochthonous paleosols on saprolite from Lower Devonian slates are Plinthosols of Cretaceous to Paleogene age with a bright pattern of red and white mottles. They occur locally, preserved below layers of Upper Oligocene basalt, tuffs and fluvial river sediments (Felix-Henningsen and Wiechmann, 1985) and show a high content (> 60 mass %) of kaolinitic clay. The sequence of a concretionary upper horizon and a mottled middle horizon, which fades with depth to a bleached, semi-terrestrial saprolite, indicates a soil development under a high groundwater table.

The paleosol of the MTV can be younger than the uppermost saprolite. In the case that a former paleosol was eroded during a climatically or tectonically induced period of denudation, the saprolite was the parent rock of a younger soil, which developed in a following phase of geomorphic stability. Paleogene and Neogene sediments of the Rhenish Massif testify to such periods of denudation of the MTV.

In the area of the Hintertaunus and the adjacent Westerwald, saprolites of the MTV are frequently exposed in open-cast mines of the clay industry, which exploits them for ceramic products, bricks and roof tiles or green house substrates, depending on the mineralogy of the exposed zones. Correlated clay sediments, which were deposited during Paleogene and Neogene erosion phases in subsiding basins of the Westerwald, are valuable kaolinitic clay deposits used for the ceramic industry.

During periglacial periods of the Pleistocene, combined processes of congelifraction, cryoturbation and solifluction as well as deposition of loess and pumice formed a sequence of superficial layers (Fig. 2). The basal layer derived from the underlying saprolite or kaolinitic paleosol. A low potential for the formation of soil structure results from the low shrinkage and swelling capacity of the kaolinitic material. Thus, the basal layer causes very unfavourable soil properties due to high bulk density, water logging, low cation exchange capacity and lack of nutrients. Therefore, the recent potentials of the soils for land use are narrowly linked to the landscape development during the past deca-million years.

3 Excursion route

The excursion proceeds from Giessen via Limburg to the Hintertaunus region. The first three sites are situated in the eastern Hintertaunus (Fig. 7):

1. A slate quarry near the village of Langhecke demonstrates characteristics and properties of fresh slates (Fig. 9).

2. The saprolite open-cast mine ”Töpferkaute” at the margin of the village of Eisenbach shows exposed terrestrial saprolite with periglacial superficial layers.

3. The saprolite open-cast mine "Ölkaute" near the village of Eisenbach shows exposed semi-terrestrial saprolite with periglacial superficial layers.

Two further sites are situated in the western Hintertaunus:

4. An autochthonous pre-Upper Oligocene Plinthosol above saprolite from Lower Devonian slates and covered by Upper Oligocene volcanic tuff, basalt and a sequence of periglacial superficial layers will be presented near the village of Biebrich.

5. An autochthonous Miocene Plinthosol, developed from alluvial sediments above quartz gravels and covered by a sequence of periglacial superficial layers, is exposed in a gravel pit near the village of Wasenbach.

4 Methods of investigation

In the following section, the procedures of physical, chemical and mineralogical soil analyses are briefly cited. They are described in detail in the method book of Blume et al. (2011). The procedure of isovolumetric balance of element masses in saprolites, which explains the mass losses and provides important information about the genesis of saprolites, is explained in detail Sect. 4.2.

4.1 Soil analytical procedures

The following analytical procedures were employed:

- *Texture of fine soil* $< 2\,mm$. After extraction of humus (H_2O_2), carbonates (HCl) and iron oxides (Na dithionite, citrate and bicarbonate) and dispersion with $Na_4P_2O_7$, the fractions were separated by wet sieving (2–0.02 mm) and a pipette method (20 to $< 2\,\mu m$).

- *Pedogenic oxides*. Amorphous Fe (Fe_o) and Mn oxides (Mn_o) were extracted with NH_4 oxalate while the total amounts of pedogenic Fe (Fe_d) and Mn oxides (Mn_d) were extracted after dissolution with Na dithionite, citrate and bicarbonate; amorphous Al (Al_l) and Si oxides (Si_l) were extracted after dissolution in 0.5 M NaOH. The concentrations of all metal ions were measured with an atomic adsorption spectrometer (AAS).

- *Total amounts of main and trace elements*. Melt tablets were analysed using XFA (X-ray fluorescence analysis; Philips PW 1480).

4.2 Isovolumetric mass balance of saprolites

Saprolites are characterized by mass losses due to dissolution of weatherable minerals, mainly silicates, followed by the export of dissolved elements with percolating pore solution or migrating groundwater. Mass losses increase with age and intensity of weathering and, thus, from the weathering front at the saprolite–rock boundary with decreasing depth towards the land surface, until all weatherable minerals are dissolved (e.g. Table 2). The increasing porosity of saprolites and the potential of the self-energizing of weathering processes result from increasing mass losses, as well as the decreasing mechanic stability of the saprolite, which makes it breakable, friable, soft and easy to erode. Therefore, bulk mass losses are an indicator for the degree of weathering, porosity and mechanic stability of a saprolite. A calculation of element mass losses (Sect. 4.2.3) indicates which elements were exported to which degree. Their geochemical behaviour allows the reconstruction of chemical processes and factors in the different saprolite zones.

4.2.1 Test on homogeneity of parent rock and saprolite with Ti / Zr ratios

The quantification of the mineralogical and geochemical differences between saprolite and parent rock requires an extensive petrological investigation of the unweathered and weathered samples. An increasing proportion of quartz sand is indicated by decreasing Ti / Zr ratios, while the opposite is the case with decreasing sand content. The contents of Ti in fresh weathered slates is 0.6 mass % ($n = 10$, SD = 0.1 %), mainly bound in rutile, which is associated with mica (Mosebach, 1954) and therefore narrowly correlated with K_t ($r = 0.92^{+++}$, $n = 10$). Zr with average concentrations of $213\,mg\,kg^{-1}$ ($n = 10$, $s = 39\,mg\,kg^{-1}$) in unweathered slates is bound in the heavy mineral zircon. With increasing contents of quartz sand, the Zr contents also increases, which causes the narrow correlation between Si_t and Zr ($r = 0.97^{+++}$, $n = 10$). On the other hand the contents of muscovite illite and the associated contents of rutile decrease with increasing contents of quartz (Si_t / K_t: $r = -0.93^{+++}$, $n = 10$; Si_t / Ti: $r = -0.91^{+++}$, $n = 10$). Therefore, the concentrations of Ti and Zr change oppositely with a change of texture of the slates and the ratios can be used as a marker of parent material homogeneity. From the Ti / Zr ratios of 150 samples of fresh slates and saprolites and determination of textural composition, a classification of textural units was possible (Felix-Henningsen, 1994):

Ti/Zr > 5	silty clay slate,
Ti/Zr 5–4	clayey silt slate,
Ti/Zr 4–2.8	sandy silt slate,
Ti/Zr < 2.8	silty sandstone and greywacke.

4.2.2 Total mass losses of saprolites

Mass losses of saprolites compared to the fresh rock result from the export of elements, released from dissolving minerals, due to leaching with percolation or groundwater. Also, mass gains are possible, which result from precipitation of dissolved elements within a saprolite zone. The determination of volume of fragments of rock and saprolite is performed by weighing fragments, saturated with penetrating oil

Table 3. Eisenbach Töpferkaute, terrestrial saprolite: bulk density (b.d.) and contents of main element oxides and LOI (mass % = g (100 g)$^{-1}$). Fe_2O_{3t} is total iron ($Fe^{III} + Fe^{II}$). LOI is loss of ignition. Of the horizons, R is fresh slate and Cj is saprolite.

Horizon	b.d. (g cm^{-3})	SiO_2 (mass %)	TiO_2 (mass %)	Al_2O_3 (mass %)	Fe_2O_{3t} (mass %)	MnO (mass %)	MgO (mass %)	CaO (mass %)	Na_2O (mass %)	K_2O (mass %)	P_2O_5 (mass %)	LOI (mass %)
Cj1	1.70	56.12	0.99	23.33	6.88	0.02	0.63	0.09	0.18	4.74	0.06	5.81
Cj2	1.70	55.28	0.99	23.07	8.13	0.05	0.57	0.10	0.10	4.31	0.11	6.24
Cj3	1.70	57.19	0.93	20.48	7.97	0.01	0.99	0.26	0.10	4.05	0.17	5.85
Cj4	1.85	58.39	0.88	19.80	7.39	0.08	2.16	0.31	0.10	4.00	0.09	5.11
Cj5	2.25	53.51	1.12	23.62	6.88	0.04	2.34	0.19	0.20	5.16	0.11	5.50
R	2.58	56.37	0.93	20.92	8.24	0.04	2.60	0.24	0.07	4.29	0.16	5.19

Table 4. Eisenbach Töpferkaute, terrestrial saprolite: bulk density (b.d. in g 100^{-1} cm^3) and volume weights of main element oxides and LOI in g vol^{-1} (vol = 100 cm^3). Fe_2O_{3t} is total iron ($Fe^{III} + Fe^{II}$). LOI is loss of ignition. Of the horizons, R is fresh slate and Cj is saprolite.

Horizon	b.d. (g vol^{-1})	SiO_2 (g vol^{-1})	TiO_2 (g vol^{-1})	Al_2O_3 (g vol^{-1})	Fe_2O_{3t} (g vol^{-1})	MnO (g vol^{-1})	MgO (g vol^{-1})	CaO (g vol^{-1})	Na_2O (g vol^{-1})	K_2O (g vol^{-1})	P_2O_5 (g vol^{-1})	LOI (g vol^{-1})
Cj1	170	95.40	1.68	39.66	11.70	0.03	1.07	0.15	0.31	8.06	0.10	9.88
Cj2	170	93.98	1.68	39.22	13.82	0.09	0.97	0.17	0.17	7.33	0.19	10.61
Cj3	170	97.22	1.58	34.82	13.55	0.02	1.68	0.44	0.17	6.89	0.29	9.94
Cj4	185	108.02	1.63	36.63	13.67	0.15	4.00	0.57	0.19	7.40	0.17	9.45
Cj5	225	120.40	2.52	53.15	15.48	0.09	5.26	0.43	0.45	11.61	0.25	12.38
R	258	145.43	2.40	53.97	21.26	0.10	6.71	0.62	0.18	11.07	0.41	13.39

Table 5. Eisenbach Töpferkaute, terrestrial saprolite: bulk mass losses (b.m.l) and individual mass losses of main element oxides and LOI in g vol^{-1} (vol = 100 cm^3). Fe_2O_{3t} is total iron ($Fe^{III} + Fe^{II}$). LOI is loss of ignition. Of the horizons, R is fresh slate and Cj is saprolite.

Horizon	b.m.l. (g vol^{-1})	SiO_2 (g vol^{-1})	TiO_2 (g vol^{-1})	Al_2O_3 (g vol^{-1})	Fe_2O_{3t} (g vol^{-1})	MnO (g vol^{-1})	MgO (g vol^{-1})	CaO (g vol^{-1})	Na_2O (g vol^{-1})	K_2O (g vol^{-1})	P_2O_5 (g vol^{-1})	LOI (g vol^{-1})
Cj1	−88	−50	−1	−14	−10	0	−6	0	0	−3	0	−4
Cj2	−88	−51	−1	−15	−7	0	−6	0	0	−4	0	−3
Cj3	−88	−48	−1	−19	−8	0	−5	0	0	−4	0	−3
Cj4	−73	−37	−1	−17	−8	0	−3	0	0	−4	0	−4
Cj5	−33	−25	0	−1	−6	0	−1	0	0	1	0	−1
R	0	0	0	0	0	0	0	0	0	0	0	0

Table 6. Eisenbach Töpferkaute, terrestrial saprolite: relative bulk mass losses (b.m.l.) and individual mass losses of main element oxides and LOI in %, related to the fresh slate. Fe_2O_{3t} is total iron ($Fe^{III} + Fe^{II}$). LOI is loss of ignition. Of the horizons, R is fresh slate and Cj is saprolite.

Horizon	b.m.l. (%)	SiO_2 (%)	TiO_2 (%)	Al_2O_3 (%)	Fe_2O_{3t} (%)	MnO (%)	MgO (%)	CaO (%)	Na_2O (%)	K_2O (%)	P_2O_5 (%)	LOI (%)
Cj1	−34	−34	−30	−27	−45	−67	−84	−75	69	−27	−75	−26
Cj2	−34	−35	−30	−27	−35	−18	−86	−73	−6	−34	−55	−21
Cj3	−34	−33	−34	−35	−36	−84	−75	−29	−6	−38	−30	−26
Cj4	−28	−26	−32	−32	−36	43	−40	−7	2	−33	−60	−29
Cj5	−13	−17	5	−2	−27	−13	−22	−31	149	5	−40	−8
R	0	0	0	0	0	0	0	0	0	0	0	0

Table 7. Eisenbach Töpferkaute, terrestrial saprolite: relative composition of bulk mass losses (r.b.m.l.) in %. Fe_2O_{3t} is total iron ($Fe^{III} + Fe^{II}$). LOI is loss of ignition. Of the horizons, R is fresh slate and Cj is saprolite.

Horizon	b.m.l. (%)	SiO_2 (%)	TiO_2 (%)	Al_2O_3 (%)	Fe_2O_{3t} (%)	MnO (%)	MgO (%)	CaO (%)	Na_2O (%)	K_2O (%)	P_2O_5 (%)	LOI (%)
Cj1	100	57	1	16	11	0	6	1	0	3	0	4
Cj2	100	58	1	17	8	0	7	1	0	4	0	3
Cj3	100	55	1	22	9	0	6	0	0	5	0	4
Cj4	100	51	1	24	10	0	4	0	0	5	0	5
Cj5	100	76	0	3	18	0	4	1	−1	−2	1	3
R	0	0	0	0	0	0	0	0	0	0	0	0

Table 8. Eisenbach Töpferkaute, terrestrial saprolite: contents of quartz in slates and saprolites as well as losses of quartz in saprolites (XDA according to Till and Spears, 1969). Of the horizons, R is fresh slate, Cv is weathered slate and Cj is saprolite. Of the neo-formed minerals, Sm is smectite, Chl-V is chlorite–vermiculite mixed layer minerals and K is kaolinite.

Horizon	Depth (m)	Neo-formed minerals	Quartz (mass %)	Quartz ($g\,100^{-1}\,cm^{-3}$)	Mass loss of quartz ($g\,100^{-1}\,cm^{-3}$)	Relative quartz loss of rock (%)
Cj1-4	2–24	K	40	74	16	18
Cj5	24–30	Chl-V	35	78	12	13
Cv	> 30	Sm	35	82	8	9
R	> 30	0	35	90	0	0

(e.g. WD 40), under submersion in water. The bulk density in $g\,cm^{-3}$ results from the ratio of the weight of the dried fragment (105 °C) and its volume. The total mass loss is indicated by the difference of bulk densities (volume weights) of fresh rock and saprolite:

$$\text{b.m.l.} = \text{b.d. rock} - \text{b.d. saprolite} \cdot 100, \quad (1)$$

where b.m.l. is mass loss ($g\,100\,cm^{-3}$) and b.d. is bulk density ($g\,cm^{-3}$).

4.2.3 Element mass losses of saprolites

A 100 % mass of rock or saprolite is geochemically defined by the sum of main element oxides (determined by XRF, X-ray fluorescence) plus the loss of ignition in mass % (Table 3).

As weathering of saprolites did not change the volume of rock, the comparison of volume-related element masses of fresh rock and saprolites is the best and only way to identify the real extent of element losses and gains in saprolites. Therefore, the masses of individual element oxides per volume (Table 4) have to be calculated as follows:

$$mE_m + LOI_m = (mE_c + LOI_c) \times \text{b.d.}, \quad (2)$$

where mE_c is the contents of main element oxide ($g\,100\,g^{-1}$ = mass %, Table 3), mE_m is the volume mass of the main element oxide ($g\,100\,cm^{-3}$ = vol %, Table 4), LOI_c is the loss of ignition (mass %), LOI_m is the volume mass of loss of ignition ($g\,100\,cm^{-3}$) and b.d. is bulk density.

Correspondingly, the masses of trace elements can be calculated and balanced.

The summarized volume masses of main elements and LOI account for the bulk density ($g\,100\,cm^{-3}$, Table 4):

$$\text{b.d.} \cdot 100 = \Sigma mE_m + LOI_m. \quad (3)$$

The differences between the volume masses of main element oxides and LOI, respectively, in rock and saprolite show the individual mass losses and gains of element oxides (and LOI) (Table 5):

$$\Delta mE_m = mE_m \text{ rock} - mE_m \text{ saprolite}, \quad (4)$$

where ΔmE_m is the mass loss or gain of element oxides ($g\,100^{-1}\,cm^{-3}$).

The total mass loss as well as individual mass losses of element oxides and LOI of saprolites (Table 5) in relation to the volume weight of element oxides and LOI, respectively, in the fresh rock (Table 4) shows the relative mass loss of element oxides (and LOI) in % (Table 6):

$$\Delta mE_m(\%) = \Delta mE_m \text{ saprolite} / mE_m \text{ rock} \cdot 100. \quad (5)$$

The individual mass loss of element oxides and LOI in relation to the bulk mass loss (Table 5) results in the relative element oxide composition of the bulk mass loss in % (Table 7):

$$\text{b.m.l.} = \Sigma \Delta mE_m / \text{b.m.l.} \cdot 100, \quad (6)$$

where b.m.l. is bulk mass loss (= 100 %) and ΔmE_m is the mass loss of main elements and LOI ($g\,100^{-1}\,cm^{-3}$).

4.3 Mineralogical methods

4.3.1 Contents and losses of quartz

Silica makes the main contribution to the bulk mass losses of elements in saprolites due to desilication, which is also an indicator for a warm humid (sub)tropical climate. Potential sources of Si are silicates and quartz. The silicate mineral in slates with the lowest weathering stability is Fe–Mg chlorite, which shows a $SiO_2 : Al_2O_3$ molar ratio of 1.99 ($n = 11$, after selective extraction with 2 N HCl, 80 °C), while kaolinite, which was newly formed from chlorite, shows a ratio of 2. Therefore, a quantitative neo-formation of kaolinite from chlorite did not lead to desilication. Furthermore, near the basis of saprolites, the neo-formation of smectites with a $SiO_2 : Al_2O_3$ molar ratio of 5.12 (Weaver and Pollard, 1973:67) after weathered chlorites indicates that the dissolution of fine grained quartz must have mainly provided the high concentration of dissolved silica. The contents of quartz was determined by XDA (X-ray diffraction and absorption) according to the procedure described in Till and Spears (1969). The contents of quartz (mass %) is converted into mass per volume ($g\,100^{-1}\,cm^{-3}$) and is isovolumetrically balanced (Table 8).

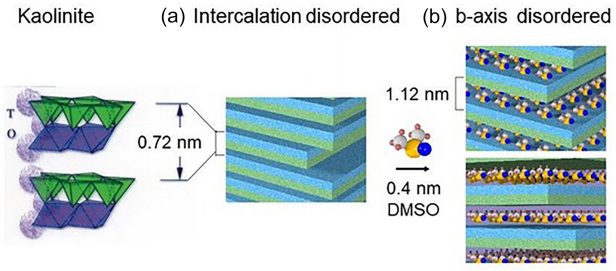

Figure 8. Two types of *b*-axis disordered kaolinites: **(a)** intercalation disordered fireclay (icd kaolinite) without intercalation of DMSO (dimethyl sulfoxide) is typical for the neo-formation in soil horizons and **(b)** *b*-axis disordered kaolinite (bad kaolinite) with DMSO intercalation is typical for the neo-formation in saprolites.

The results show that dissolution and leaching of up to 18 % of the original quartz content in the fresh slate largely contributed to the loss of silica and the bulk mass loss of saprolites.

4.3.2 Contents of clay minerals and crystallinity of kaolinite

The contents of kaolinite as the neo-formed mineral after Fe–Mg chlorite (and in part smectite) was determined according to Islam and Lotse (1986). The contents of kaolinite were calculated from the amount of extracted Al after dissolution of the clay fraction in 0.5 N NaOH (80 °C, 3 min).

All clay minerals were determined by X-ray diffraction (XRD) of oriented specimen of the natural clay fraction < 2 µm, dispersed in water, before and after saturation with ethylene glycol, K^+, fumigation with DMSO (dimethyl sulfoxide) and heating (1 h 450 and 550 °C).

Well-ordered kaolinites can be identified by a peak-triplet at 20–25° 2θ in X-ray diffraction diagrams (Cu radiation). Such kaolinites occur as white monomineralic precipitates and filling of veins in semi-terrestrial saprolites. Kaolinites of paleosols and saprolites (references in Felix-Henningsen, 1990, 2015), which mainly developed topotactically during the alteration of primary silicates, belong to the less ordered type of *b*-axis disordered kaolinites and fireclay minerals. These fractions can be distinguished by the expansion after intercalation with DMSO. As a result of fumigation of an oriented XRD clay specimen (70 °C for 72 h) with DMSO, well-crystalline and *b*-axis disordered kaolinites, which are abundant (> 90 %) in saprolites, expand from 0.72 to 1.12 nm (Fig. 8).

On the contrary, the clay fraction (> 60 mass %) of the paleosol shows an increasing proportion (up to 90 %) of fireclay from the saprolite to the former topsoil. Fireclay does not expand after treatment with DMSO (Fig. 8). Therefore, DMSO intercalation allows the sources of kaolinites (from saprolites) and fireclay (from paleosol) in sediments to be identified, and the results support the geomorphological reconstruction of landscape development.

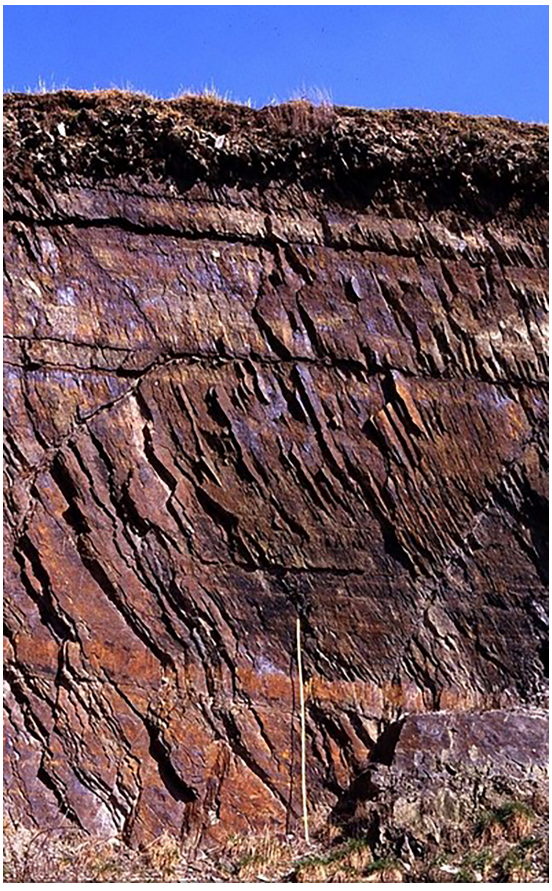

Figure 9. Fresh slate of the Rhenish Massif with nearly vertical cleavage planes, covered by a layer of rock fragments due to periglacial congelifraction, exposed at the bottom of a valley in the eastern Hunsrück. In such deeply incised valleys the MTV has been completely eroded.

5 Excursion sites

5.1 Village of Langhecke: fresh slates

Clastic sedimentary rocks developed from shallow marine sediments of the Lower Devonian and have the largest extension in the Rhenish Massif. As a consequence of diagenesis and anchi-metamorphosis during the Variscian orogenesis, the pelitic sediments, 5–10 km thick, were transformed to folded clay and silt slates, while intercalated banks of greywacke sandstones originated from sand sediments (Fig. 9). Due to the diagenetic transformation of silicate minerals during the Variscian orogenesis, released silica was concentrated in milky quartz veins. Detritic organic matter of the marine sediments changed to coaly bituminous substances, which cover the surfaces of phyllosilicates and cause the black colour of the slates. Also in the Hintertaunus re-

Figure 10. Periglacial congelifraction of the fresh slate and lateral movement by solifluction led to a horizontal orientation of the slate fragments and formed the basal layer.

gion, Lower and Middle Devonian clay and silt slates, intercalated with banks of greywacke and greenstone, served as parent rock of the MTV.

The occurrence of fresh slates near the recent land surface is bound to the extent of Tertiary and Quaternary denudation of the MTV, which is up to 150 m thick. In the central and most uplifted areas (∼ 450–900 m a.s.l.) of the Rhenish Massif the weathering mantle was largely removed. Because of congelifraction of the exposed slate and solifluction, a basal layer of slate fragments developed during Quaternary periglacial periods, covered by a thin Late Pleistocene main layer of redistributed loess and pumice (Fig. 10).

In the less tectonically uplifted (∼ < 450 m a.s.l.) lower and marginal zones of the mountainous region with thick remnants of the MTV, fresh slates only occur at the bottom of deeply incised erosion valleys (Fig. 11). As the clay slates of the Rhenish Massif have been used since Roman times as cover for roofs and walls of houses, they have been mined in open-cast and subsurface mines until today.

The excursion site at village of Langhecke shows an example of the occurrence of fresh slates, exposed in a former

Figure 11. Remnant of the Palaeogene planation plane in ∼ 300 m a.s.l. of the Hintertaunus (Rhenish Massif), dissected by Neogene and Quaternary regressive erosion. Fresh slates are only exposed at the valley bottom.

slate mine at the bottom of such an erosion valley. They display characteristics as described in the following points.

- Bulk densities are measured to be 2.50–2.58 g cm^{-3} for clay slates and 2.67–2.69 g cm^{-3} for silt slates.
- Mineralogical composition of slate is as follows:
  - 35–45 mass % muscovite, $KAl_2(AlSi_3O_{10})(OH_2)$;
  - 25–35 mass % Fe–Mg chlorite (Fe–rhipidolite), composed of $(Mg^{2+}_{2.12}\ Fe^{2+}_{2.16}\ ME^{3+}_{1.72})\ (Si_{2.28}Al_{1.72})\ O_{10}\ (OH)_8$; the distribution of central ions was modelled according to Brindley and Gillery (1956) and Makumbi and Herbillon (1975);
  - 25–35 mass % quartz, and in greywacke up to 90 mass %;
  - < 1 mass % accessory minerals of pyrite and apatite;
  - 0.3–0.5 mass % C coaly bituminous organic carbon;
  - heavy minerals, consisting of an ultra-stable group with zircon, tourmaline and rutile.

5.2 Eisenbach Töpferkaute: terrestrial saprolite from slates

The open-cast clay mine Töpferkaute at the margin of the village of Eisenbach is situated at the north-west-exposed middle slope of the River Eisenbach valley (Fig. 6), which already started to incise during the Tertiary, and about 60 m below the remnant of a planation plain on which the Eisenbach Ölkaute excursion site is situated (see Sect. 5.3).

5.2.1 Saprolite

The profile, 25 m deep, exposes a terrestrial saprolite from fresh and nearly fresh slate to the upper, strongly weathered

Table 9. Eisenbach Töpferkaute: profile of a terrestrial saprolite of the Mesozoic–Tertiary weathering mantle, covered by Pleistocene periglacial layers. Horizon symbols and characterization are according to AG Bodenkunde (2005). Depth refers to the lower boundary. Location: village of Eisenbach. TK25: 5615 Villmar r 3447581 h 5579187; 250 m a.s.l. Relief: lower middle slope. WRB: (Stagnic) Luvisol.

Hor. no.	Horizon symbol	Depth (cm)	Horizon characteristics
1	Ai + Ah	5	Main layer from loess mixed with pumice, disturbed humic topsoil, dark brown (10YR 4/3), silty loam (Lu), weakly humic, strongly rooted, crumb structure, low bulk density, diffuse transition
2	Al + Bt	90	Main layer from loess mixed with pumice, yellowish brown (10YR 5/8), strong clayey silt (Ut4, G2), very weak humic, middle rooted, polyhedral to platy structure, low to middle bulk density, wavy lower boundary
3	II Sw	110	Middle layer from loess, yellowish brown (10YR 5/6), strong clayey silt (Ut4, fX1), weakly rooted, coherent structure, high bulk density, single Bt bands with accumulation of oxides, wavy lower boundary
4	III Sd	140	Basal layer from redistributed saprolite, brown (10YR 5/8), weak clayey loam (Lt2, fX2), weakly rooted, weak rusty mottling, polyhedral structure, high bulk density, sharp wavy lower boundary
5	Bv1	170	Basal layer from redistributed saprolite, brown (10YR 5/8), silty clay (Tu3, fX1), prism structure, high bulk density
6	Bv2	200	Basal layer from redistributed saprolite, reddish brown (7.5YR 6/8), clayey loam (Lt3, fX1), prism structure, high bulk density, sharp lower boundary
7	IV mCj1	1000	Mesozoic–Tertiary saprolite from silt slate, red (2.5YR 5/6) and purple zones (7.5R 5/3) interfingered with yellow brown (10YR 7/6) to dark brown (10YR 5/8) zones, following the cleavage and joints, soft and friable, with black Mn oxide stains on cleavage plains
8	mCj2	1500	Mesozoic–Tertiary saprolite from silt slate, reddish brown (7.5YR 7/6), red (2.5YR 7/6) and red-purple (10R 5/3) zones; soft, to disintegrate manually
9	mCj3	2000	Mesozoic–Tertiary saprolite from silt slate, brownish yellow (10YR 7/6), sections with quartz veins are interfingered with mCj2 over a depth of 5–8 m, cleavage plains stained with black-brown Mn oxides; indurated, but plates centimetres thick are manually breakable
10	mCj4	2400	Mesozoic–Tertiary saprolite from silt slate, light olive-grey (5BG 7/1), only apart from joints and fissures dark grey (10BG 5/1) zones with higher contents of primary coaly bituminous organic matter, cleavage plains with dark brown to black coatings of Fe-Mn oxides
11	mCj5	3000	Mesozoic–Tertiary saprolite from silt slate, basal zone with vertical zones of olive-grey (10BG 5/1), weakly oxidized saprolite interfingered with black (N 3/0) fresh slate, massive
12	mCn	3000+	Nearly fresh silt slate, black (N 3/0), matrix along single joints and quartz veins with olive elucidation due to oxidation (10G 4/1)

Table 10. Eisenbach Töpferkaute: texture of the fine earth (< 2 mm), free of humus and carbonates (texture analyses of saprolite were performed with ground material; therefore the data present the relative disintegration but not the real particle size of the original slate texture). Fractions: c, m and f are coarse, middle and fine; S is sand, U is silt and T is clay. Depth refers to the lower boundary.

Horizon	Depth (cm)	Texture (mass %)						
		cS	mS	fS	cU	mU	fU	T
Ai + Ah	5	2.33	2.54	4.61	36.29	21.63	8.21	24.40
Al + Bt	90	0.95	1.59	2.77	39.22	23.04	7.97	24.46
II Sw	110	1.83	2.27	3.72	40.84	24.77	8.75	17.82
III Sd	140	5.93	5.99	7.80	20.97	19.67	8.91	30.73
Bv	170	1.67	1.64	2.87	27.43	20.88	9.10	36.41
Bv2	200	2.62	2.95	6.64	17.75	14.55	11.43	44.06
IV mCj1	1000	1.32	4.05	8.49	12.19	21.67	29.70	22.58
mCj2	1500	25.80	23.58	12.27	6.88	11.92	13.34	6.21

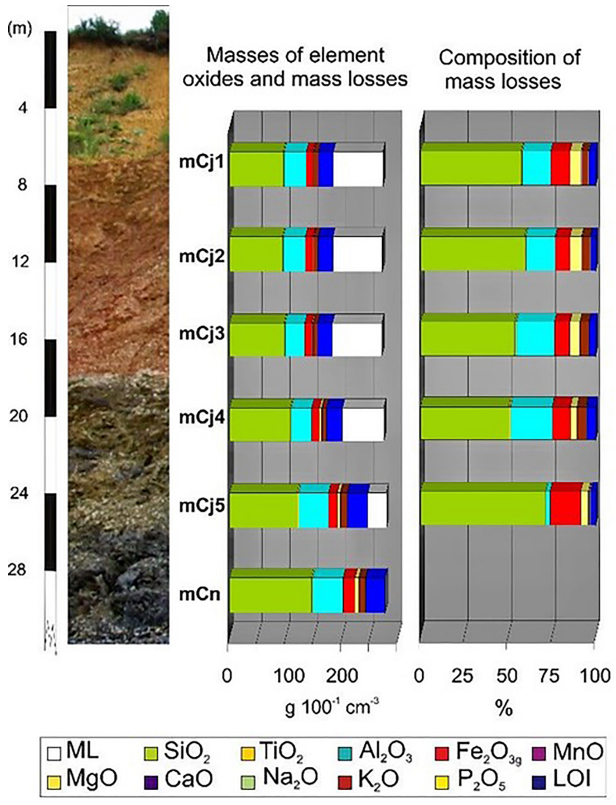

Figure 12. Eisenbach Töpferkaute, terrestrial saprolite: main element composition volume weight (vol-wt) in g 100^{-1} cm^{-3}) of fresh slate and saprolite, isovolumetric bulk mass losses (ML) and relative elemental composition of mass losses (in % of the bulk mass loss).

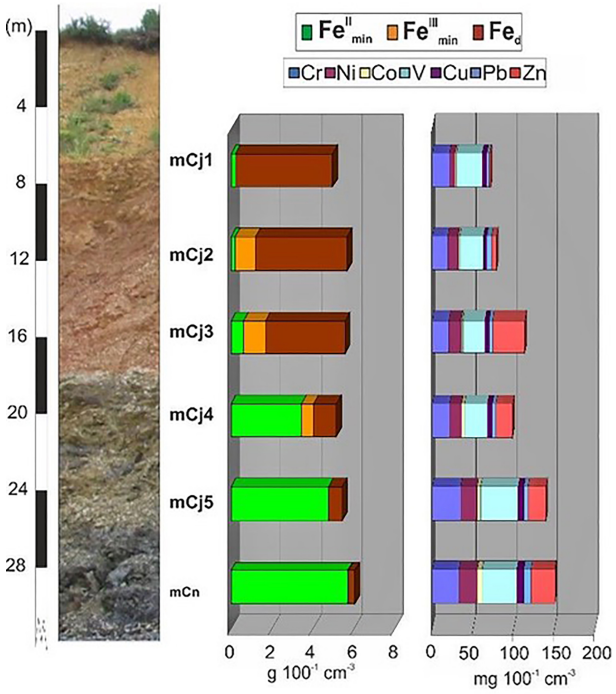

Figure 13. Eisenbach Töpferkaute, terrestrial saprolite: volumetric masses of iron fractions (mineralogically bound Fe^{III}_{min} and Fe^{II}_{min}, as well as free iron oxides Fe_d) and trace elements of fresh slate and saprolite.

zones. The individual zones are interfingered over distances of many metres. Interfingering is a typical phenomenon in deep weathered slates because the more or less steep inclined to vertical cleavage planes and tectonic joints cause differences in permeability and weathering intensity between jointed and massive parts of the slate.

In the lowermost saprolite zone (Cj5, Table 9), the black-grey colour of the slate changes to an olive colour along cleavage plains and joints as a consequence of oxidation, which increases to the upper saprolite zones (Cj4, Table 9). The loss of primary coaly bituminous organic matter follows the penetration of air into the rock matrix and indicates an increase of porosity in the wake of dissolution of minerals and export of dissolved elements. This is confirmed by mass losses (Fig. 14) as well as the loss of mechanical stability. Within the olive-coloured parts, inner crystalline oxidation transformed the primary chlorites to chlorite–vermiculite mixed layer (m.l.) minerals, which occur beside kaolinite. The Stephan Schmidt KG mines this saprolite zone for use as a greenhouse substrate. The colour of the higher saprolite zones (Cj1–Cj3, Table 9) changes to brown, light and dark red and purple-red, as all iron-bearing silicates weathered completely, and free iron oxides, which precipitated as goethite and hematite, were formed.

Leaching of elements by percolation water under oxidizing conditions caused mass losses of 25–30 % of the original rock mass (Fig. 12) and a loss of stability of the saprolite, which changed to a soft, friable material. Especially Si, Al, bases and to a minor extent also Fe contributed to the mass loss. The loss of dissolved SiO_2 and bases was a consequence of weathering of silicates and leaching of dissolved elements under warm (sub)tropical climatic conditions, as the mobility of silica depends only on the temperature of the weathering solution. Because of the desilication the amorphous Si fraction of the saprolite is impoverished relatively to the contents of amorphous Al compounds (Table 11). The losses of total Al_2O_3 (Fig. 12), dependent on acid conditions ($pH < 4.5$) and complexation by dissolved organic matter, increased above the lowermost saprolite zone, as the buffer capacity decreased after the leaching of bases. This also shows that Al, released from the primary silicates, was not quantitatively captured in neo-formed kaolinite. Restricted to the lowermost saprolite (Cj5, Fig. 12), Fe_2O_3 contributes to the mass loss as intermittent waterlogging above the massive fresh slate supported the mobilization of iron under reducing conditions. In the upper saprolite zones (Cj1–4, Fig. 12) the mass loss of iron does not increase any more as the oxidizing conditions caused the formation of immobile oxides.

Table 11. Eisenbach Töpferkaute: contents of pedogenic oxides. Depth refers to the lower boundary.

Horizon	Depth (cm)	Fe_o (mg g^{-1})	Fe_d (mg g^{-1})	Fe_o / Fe_d	Mn_d (mg g^{-1})	Si_l (mg g^{-1})	Al_l (mg g^{-1})
Ai + Ah	5	1.65	13.88	0.12	0.45	5.12	6.60
Al + Bt	90	1.96	13.44	0.15	0.44	6.16	8.41
II Sw	110	2.09	11.66	0.18	0.65	6.28	6.74
III Sd	140	1.64	28.17	0.06	0.47	7.91	10.96
Bv	170	1.26	21.27	0.06	0.40	6.74	7.98
Bv2	200	0.44	33.14	0.01	0.08	8.95	11.34
IV mCj1	1000	0.19	47.41	0.00	0.32	1.79	6.42
mCj2	1500	0.29	44.90	0.01	0.07	2.32	7.32
mCj3	2000	0.32	38.90	0.01	0.04	2.23	5.11
mCj4	2400	0.34	11.03	0.03	0.22	2.69	2.79
mCorj	3000	0.30	6.57	0.05	0.02	2.13	2.50
mCn	> 3000	0.33	0.45	0.73	0.01	1.87	1.30

Table 12. Eisenbach Töpferkaute: clay mineral composition. LM is labile minerals > 1.8 nm, Sm is smectite, WL is mixed layer minerals, Chlp is primary chlorite, Chls is secondary (Al–)chlorite, Ver is vermiculite, Ill is illite, Kao icd is fireclay and Kao bad is *b*-axis disordered kaolinite; n.n. refers to values that are not detectable. Depth refers to the lower boundary.

Horizon	Depth (cm)	Clay minerals < 2 µm (mass %)[a]									
		LM	Sm	WL	Chlp	Chls	Ver	WL	Ill	Kao icd	Kao bad
Ai + Ah	5	5	4	4	n.n.	n.n.	n.n.	n.n.	56	11	25
Al + Bt	90	4	4	4	n.n.	n.n.	5	11	37	15	24
II Sw	110	14	n.n.	n.n.	n.n.	n.n.	5	7	33	11	28
III Sd	140	n.n.	7	7	n.n.	n.n.	6	9	40	11	28
Bv1	170	8	8	n.n.	n.n.	n.n.	11	n.n.	30	14	28
Bv2	200	n.n.	n.n.	5	n.n.	n.n.	9	n.n.	38	20	28
IV mCj1	1000	n.n.	n.n.	n.n.	n.n.	n.n.	n.n.	n.n.	79	n.n.	21
mCj2	1500	n.n.	n.n.	n.n.	n.n.	n.n.	n.n.	n.n.	75	n.n.	25
mCj3	2000	4	n.n.	n.n.	n.n.	n.n.	n.n.	n.n.	76	n.n.	20
mCj4	2400	4	n.n.	n.n.	22[b]	n.n.	n.n.	4	58	n.n.	12
mCj5	3000	1	n.n.	n.n.	20[b]	n.n.	n.n.	1	73	n.n.	6
mCn	> 3000	2	n.n.	n.n.	12	n.n.	n.n.	n.n.	82	n.n.	4

[a] Masses calculated with reflex intensity × factor (Tributh and Lagaly, 1989). [b] Apparent increase of mass, due to increase of reflex intensity with formation of chlorite–vermiculite m.l. minerals.

The iron balance (Fig. 13) shows that Fe^{II}, bound within the chlorite minerals of the fresh slate, was successively oxidized from Cj5 upwards to Cj1. A first step of inner-crystalline oxidation was followed by the release of Fe ions from chlorites and precipitation as pedogenic (free) iron oxides. Their contents rise continuously from the fresh rock to the uppermost saprolite zone with increasing intensity of weathering of silicates (Table 11). Mn oxides are irregularly distributed as their better solubility under acid conditions promoted diffusive redistribution in phases of water saturation of the saprolite matrix under weak reducing conditions and accumulation on joint plains under oxidizing conditions. A total of 50 % of the original volume weight of heavy metals, also mainly bound in chlorite minerals as a substitute for Fe, was leached from the saprolite according to their relative solubility under acid conditions (Fig. 13).

The clay mineral association (Table 12) shows a transformation of chlorites of the fresh slate to chlorite–vermiculite mixed-layer minerals within the olive-grey parts along joints of the lowermost saprolite zone as well as in the olive-grey saprolite. This shows that the weathering of primary silicates as well as leaching of silica and bases is accompanied by the oxidation of the primary coaly bituminous organic matter of the slates.

As the saprolite, exposed in 70 m higher altitude at the Ölkaute excursion site (see Sect. 5.3), was formed under groundwater saturation, the saprolite of the Töpferkaute developed obviously during a younger stadium of deep weathering, perhaps during the Miocene. The tectonical uplift of the Hintertaunus during the Upper Oligocene caused the lowering of the groundwater table and erosion of the Cretaceous to Paleogene saprolite. Therefore, deep weathering contin-

ued under terrestrial conditions during the middle Miocene warm humid period.

5.2.2 Periglacial layers and Holocene soil

The saprolite is covered with periglacial layers up to several metres thick, which are the parent material of the Holocene Stagnic Luvisol. The analytical data are displayed in Tables 10–12. The basal layer consists of material from the uppermost saprolite zone, redistributed by solifluction, covered by a middle layer of loess and an uppermost main layer of loess mixed with pumice of the Late Pleistocene Laacher See eruption (Table 9). Therefore, the texture of the middle and upper layer is rich in coarse silt, typical of the large proportion of loess. The basal layer shows high clay contents as a consequence of intensive periglacial congelifraction of redistributed saprolite material and the admixture of substrate of a periglacially reworked paleosol rich in kaolinitic clay, which is indicated by the high total amounts of kaolinite in the clay fraction (Table 12). They also contain weakly weathered three-layer silicates, which in the main and middle layers derive from loess. In the basal layer, they originate from redistributed material of less weathered, lower saprolite zones, which were exposed by denudation in upslope areas. Due to congelifraction, cryoturbation and lateral transport the material was admixed to solifluction layers.

5.3 Eisenbach Ölkaute: semi-terrestrial saprolite from slates, paleosol sediment and Vallendar gravel

5.3.1 Saprolite

Since 1866, white, bleached saprolite has been mined in the Ölkaute quarry, near the village of Eisenbach, as raw material for the ceramic industry. The exposed saprolite from silt slate (Table 13) presents the transition of the bleached horizon (mCewj), up to 10 m thick, to a grey saprolite (mCorj) and further down a black-coloured saprolite (mCrj). In both zones the undisturbed rock structure of the slates is preserved, although the saprolite is strongly weathered, friable and can be disintegrated manually. According to the pedogenic iron forms (Table 15) and clay mineralogical composition (Table 16) differences between the saprolite zones exist.

The white colour of the mCewj zone (Figs. 15 and 16) proves that the dissolution of all iron-bearing silicates and the formation of kaolinite, as well as the leaching of bases, silica and metal ions must have occurred under reducing conditions as a result of saturation with migrating ground water. Therefore, Fe and Mn ions, released from silicates, remained mobile and were completely leached with a lateral groundwater flow. The decay of the primary organic matter in the bleached horizon, which until today is still present in the lower saprolite zone with sustainable reducing conditions, is a consequence of oxidation after the lowering of the groundwater table. This went along with the tectonic uplift of the Hintertaunus area and regression of the nearby sea since the

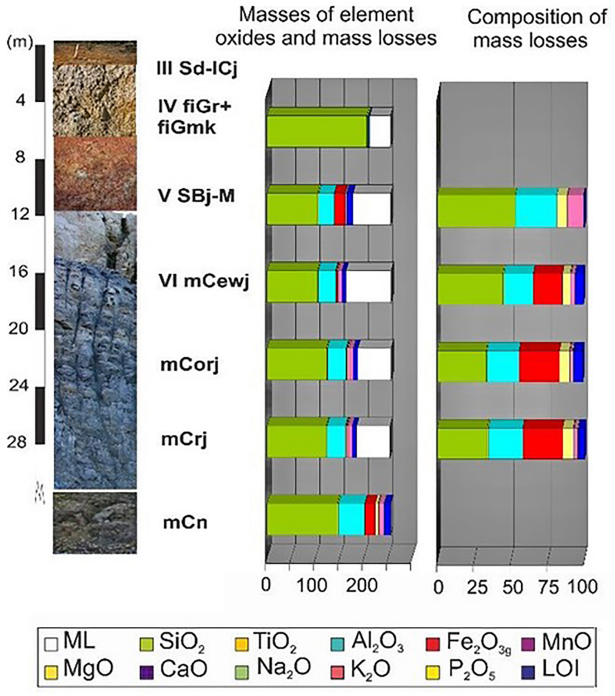

Figure 14. Eisenbach Ölkaute, semi-terrestrial saprolite: main element composition (vol-wt in $g\,100^{-1}\,cm^{-3}$) of fresh slate and saprolite, isovolumetric bulk mass losses (ML) and relative elemental composition of mass losses (in % of the bulk mass loss).

Figure 15. Eisenbach Ölkaute: soft, white bleached saprolite from silt slate (MTV) with well-preserved slate structure.

Upper Oligocene. In addition, arid climatic phases existed during the Upper Oligocene and Lower Miocene and led to the formation of silcretes in Tertiary river sediments of the Rhenish Massif, as demonstrated in the Ölkaute. The deep exsiccation of the saprolite must have contributed to the oxidation of the upper zones of the saprolite.

Table 13. Eisenbach Ölkaute: synthetic profile of a semi-terrestrial saprolite of the Mesozoic–Tertiary weathering mantle, covered by an Upper Oligocene soil sediment and fluvial sediments as well as Pleistocene periglacial layers. Horizon symbols and characterization are according to AG Bodenkunde (2005). Depth refers to the lower boundary. Location: north of the village of Eisenbach. TK25: 5613 Schaumburg r 3446728 h 5580017; 290 m a.s.l. Relief: plateau, weakly inclining to the west. WRB: Stagnic Luvisol

Hor. no.	Horizon symbol	Depth (cm)	Horizon characteristics
1	L + Of	2–0	Humic layer
2	Ah	0–6	Main layer from loess mixed with pumice, humic horizon, grey-brown (10YR 3/4) silty loam (Lu), humic, rooted, low bulk density, crumb structure, sharp lower boundary
3	Al	25	Main layer from loess mixed with pumice, yellowish brown (10YR 4/4) sandy loam (Ls3), weak humic, weakly rooted, smooth transition
4	S-Bt	48	Main layer from loess mixed with pumice, pale brown (10YR 4/3) silty loam (Lu), weakly rooted, dark brown clay cutans, Mn oxide concretions, polyhedral structure, sharp horizontal boundary
5	II S-Bt	78	Middle layer, dominated by loess, yellow-brown (10YR 6/6) clayey silt (Ut3), weakly rooted, dark brown (10YR 5/4) clay cutans, Mn oxide concretions, polyhedral to prismatic structure, sharp and wavy lower boundary
6	III Sd-lCj	113	Base layer, grey (10YR 7/2) and yellowish brown (10YR 5/4) loamy clay (Tl) coherent structure, high bulk density, wavy lower boundary
7	IV fiGr + fiGmk	700	Fluvial sediment (Upper Oligocene Vallendar gravel), more or less silicified white (10Y 8/1) sand with layers of sandy silt (Us, G3+Ls3), weakly rounded milky quartz pebbles and boulders, layers of massive silcrete
8	V SBj-M1	1000	Soil sediment (redistributed Plinthosol) of a pre-Upper Oligocene paleosol as filling of an erosion gully, red (2.5YR 3/4) and weakly grey mottled (5BG 7/1) loamy clay (Tl3) to clay (Tt)
9	SBj-M2	1300	Soil sediment (redistributed Plinthosol) of a pre-Upper Oligocene paleosol as filling of an erosion gully, grey (10BG 7/1), rusty mottled (10R 3/4) clay (Tt)
10	VI mCewjs	1500	Transition zone in Mesozoic–Tertiary saprolite of silt slate at the gully margin, brownish yellow (10YR 8/4), soft
11	mCewj	1900	Mesozoic–Tertiary saprolite of silt slate, white (10BG 6/1), soft, yellow and orange stains of iron oxide
12	mCorj	2100	Mesozoic–Tertiary saprolite of silt slate, light grey (5BG 8/1), soft, yellow and orange stains of iron oxide
13	mCrj	2500+	Mesozoic–Tertiary saprolite of silt slate, dark grey (5B 5/1), soft

Table 14. Eisenbach Ölkaute – texture of the fine earth (< 2 mm), free of humus and carbonates (texture analyses of saprolite were performed with ground material; therefore the data present the relative disintegration but not the real particle size of the original slate texture). Fractions: g, m and f are coarse, middle and fine; S is sand, U is silt and T is clay. Depth refers to the lower boundary.

Horizon	Depth (cm)	Texture (mass %)						
		cS	mS	fS	gU	mU	fU	T
Ah	6	0.54	8.27	15.34	19.76	20.71	12.19	23.19
Al	25	0.34	9.49	16.64	18.04	4.49	29.62	21.38
S-Bt	48	1.06	12.74	18.71	18.52	16.22	12.48	20.27
IIS-Bt	78	1.14	2.19	8.37	18.49	16.49	11.10	42.22
IIISd-lCj	113	0.61	1.84	8.12	11.99	13.14	9.48	54.82
IVfiGr	700	11.68	12.36	16.46	18.37	20.26	13.95	6.72
VSBj-M1	1000	0.90	0.86	0.61	3.81	9.82	11.83	72.17
SBj-M2	1300	1.36	1.27	1.89	5.15	12.26	10.63	67.44
VImCewjs	1500	0.04	0.40	2.75	16.56	22.20	23.30	34.75
mCewj	1900	0.31	0.94	4.96	20.61	21.88	22.09	29.21
mCorj	2100	0.04	0.95	2.75	23.18	22.46	20.85	29.77
mCrj	2200+	0.01	0.27	4.13	26.32	24.83	19.82	24.63

Figure 16. Eisenbach Ölkaute, white bleached saprolite from silt slate (MTV) with an erosion gully (Upper Oligocene?), refilled with red, white mottled soil sediment of a former Plinthosol.

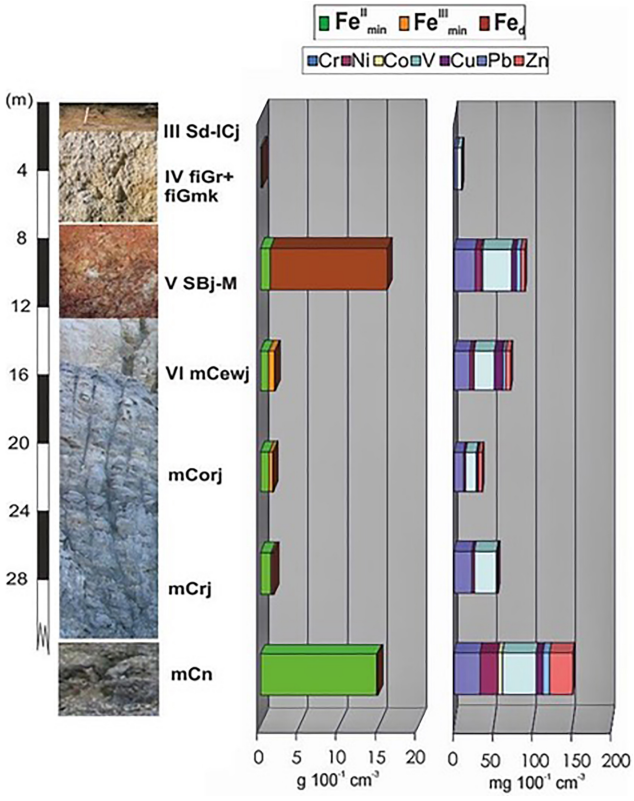

Figure 17. Eisenbach Ölkaute, semi-terrestrial saprolite: volumetric masses of iron fractions (mineralogically bound Fe^{III}_{min} and Fe^{II}_{min}, as well as free iron oxides Fe_d) and trace elements of fresh slate and saprolite.

Bulk mass losses are clearly higher within the bleached and reduced zones (Fig. 14) than in the terrestrial saprolite of Eisenbach Töpferkaute (Fig. 12). Because of leaching under reducing conditions, iron and other metal ions are strongly depleted (Fig. 17). Therefore, iron oxide contributes more than 25 % to the bulk mass loss. The relative proportion of SiO_2 in the bulk mass loss increases from the lower to the uppermost saprolite zone and indicates the increase of desilication. As only the illite minerals weathered to kaolinite while muscovite remained stable, the losses of K_2O are rather low.

5.3.2 Soil sediment

A former erosion gully, several metres deep (Fig. 16), which extended from the former plantation plain downwards to a valley, cut through the bleached saprolite and was filled with soil material of a red-white mottled Plinthosol after the soil has been undercut by linear erosion of the soft saprolite. It broke down and was mixed with fragments of the bleached saprolite. The paleosol material has a clay content around 70 mass % (Table 14), typical of Cretaceous–Paleogene fersiallitic paleosols. The reason for such a high clay content is the weathering of muscovite remaining stable within the saprolite and the transformation to kaolinite (65–70 mass %) and illite (30–35 mass %). Up to 50 % of the kaolinite fraction consists of fireclay. The negligible contents of fireclay within the saprolite shows that the formation of fireclay is typically bound to fersiallitic and ferrallitic paleosol horizons, which were subject to strong desilication.

From the characteristics of the soil sediment and the analytical data the processes of soil formation, such as acidification, weathering of silicates and desilication and neoformation of kaolinite, can be concluded. The isovolumetric balance shows that the volumetric contents of Fe_2O_3 in the soil sediments match those of the fresh slate (Fig. 14). Iron obviously was not leached from the paleosol. This could be a consequence of permanent oxidizing conditions within the soil zone, which did not allow an enhanced mobility of iron. The fact that the underlying saprolite is nearly free of mineralogically bound iron and completely depleted in free iron oxides leads to two hypotheses:

a. If bleached saprolite became the parent material of the soil after phases of erosion of previous soils (e.g. due to

Table 15. Eisenbach Ölkaute: contents of pedogenic oxides. Depth refers to the lower boundary.

Horizon	Depth (cm)	Fe_o (mg g^{-1})	Fe_d (mg g^{-1})	Fe_o / Fe_d	Mn_d (mg g^{-1})	Si_l (mg g^{-1})	Al_l (mg g^{-1})
Ah	6	3.24	7.49	0.43	0.42	11.98	11.11
Al	25	2.90	7.70	0.38	0.63	11.74	13.16
S-Bt	48	2.33	9.87	0.24	1.32	16.86	20.10
IIS-Bt	78	0.55	12.36	0.04	0.23	8.72	9.97
IIISd-lCj	113	0.12	9.17	0.01	0.02	10.81	15.42
IVfiGr	700	0.04	0.25	0.16	0.01	0.60	1.93
VSBj-M1	1000	0.76	82.58	0.01	0.03	3.02	8.35
SBj-M2	1300	0.20	20.22	0.01	0.02	2.11	7.08
VImCewjs	1500	0.13	21.19	0.01	0.09	1.59	5.88
mCewj	1900	0.05	0.73	0.06	0.01	2.84	2.21
mCorj	2100	0.05	0.28	0.17	0.01	3.04	1.99
mCrj	2200+	0.16	1.20	0.13	0.01	2.87	1.42

Table 16. Eisenbach Ölkaute: clay mineral composition. LM is labile minerals > 1.8 nm, Sm is smectite, WL is mixed layer minerals, Chlp is primary chlorite, Chls is secondary (Al–)chlorite, Ver is vermiculite, Ill is illite, Kao icd is fireclay and Kao bad is *b*-axis disordered kaolinite; n.n. refers to values that are not detectable. Depth refers to the lower boundary.

Horizon	Depth (cm)	Clay minerals < 2 µm (mass %)*									
		LM	Sm	WL	Chlp	Chls	Ver	WL	Ill	Kao icd	Kao bad
Ah	6	2	n.n.	n.n.	n.n.	n.n.	n.n.	n.n.	64	10	25
Al	25	4	n.n.	n.n.	n.n.	n.n.	4	n.n.	58	14	21
S-Bt	48	4	n.n.	n.n.	n.n.	n.n.	n.n.	n.n.	59	13	24
IIS-Bt	78	6	n.n.	n.n.	n.n.	n.n.	n.n.	n.n.	39	28	27
IIISd-lCj	113	n.n.	n.n.	n.n.	n.n.	n.n.	n.n.	n.n.	27	52	22
IVfiGr	700	n.n.	n.n.	n.n.	n.n.	n.n.	n.n.	n.n.	0	68	32
VfSBj-M1	1000	n.n.	n.n.	n.n.	n.n.	n.n.	n.n.	n.n.	35	28	37
fSBj-M2	1300	n.n.	n.n.	n.n.	n.n.	n.n.	n.n.	n.n.	32	37	32
VImCewjs	1500	n.n.	n.n.	n.n.	n.n.	n.n.	n.n.	n.n.	65	2	32
mCewj	1900	n.n.	n.n.	n.n.	n.n.	n.n.	n.n.	n.n.	73	2	24
mCorj	2100	n.n.	n.n.	n.n.	n.n.	n.n.	n.n.	n.n.	75	2	22
mCrj	2200+	n.n.	n.n.	n.n.	n.n.	n.n.	n.n.	n.n.	75	3	22

* Masses calculated with reflex intensity × factor (Tributh and Lagaly, 1989).

Paleogene climate changes or tectonic uplift), the contents of iron oxides must have been supplied by precipitation of iron in the capillary seam of the groundwater. This seems to be less possible, as the saprolite below is completely depleted in iron, which means that the iron concentration of the groundwater was extremely low.

b. The high iron content of the paleosol results from the weathering of the fresh slate under terrestrial conditions at the beginning of the formation of the weathering mantle and before the saprolite with the groundwater body was formed. According to this, during the whole period of formation of the weathering mantle, the soil surface was stable and little erosion took place. In the case of erosion, the primarily formed soil horizon was removed with time and the bleached saprolite became the parent material. This remains to be an unresolved question.

5.3.3 Silicified fluvial sediment

The western wall of the saprolite open-cast mine cuts a bank of fluvial sediments, superimposing the soil sediment fill of the former erosion gully and the adjacent bleached saprolite. The sediments consist of partly silicified and cemented pure quartz sand with gravel of well-rounded milky quartz, which derived from erosion of less weathered primary quartz veins within the saprolite. Less rounded boulders of Taunus quartzite, up to 40 cm in diameter, indicate a long distance transport of the fluvial sediments because the next sources of Taunus quartzite are located more than 3 km away in a south–south-east direction. They must have been sedimented in the Upper Oligocene Vallendar river system on the Pale-

ogene planation plain, before the tectonic subsidence of the fault blocks and the incision of the Late Tertiary and Quaternary valleys, separating the planation plane around Ölkaute from the High Taunus. The isovolumetric balance of elements (Fig. 14) shows a strong absolute accumulation of silica, indicating silification as a consequence of (semi-)arid climate conditions, which existed throughout Middle Europe in the transition from the Upper Oligocene to the Lower Miocene.

5.3.4 Periglacial layers and Holocene soil

The uppermost layers, 2 m thick, above the Tertiary fluvial sediments consist of periglacial layers, organized in basal, middle and main layers (Table 13).

The basal layer is free of loess but rich in clay (Table 14) and consists of a more or less brown to white loam, which derived from congelifraction of the saprolite. During thaw periods the porous saprolite was saturated with water, which caused rapid congelifraction during the frost periods. The disintegration of kaolinite aggregates (booklets), which tend to develop as pseudomorphoses of weathered silicates, severely enhanced the clay content. Admixture of saprolite zones and paleosol material increased the contents of pedogenic iron. The contents of amorphous silica and aluminum correlate with the contents of clay (Table 15). The middle layer is dominated by loess but contains also a proportion of material of the basal layer, rich in clay. The pedogenic SBt horizon characterizes a Stagnic Luvisol. Micromorphological analyses show that the majority of the clay cutans were destroyed by periglacial frost pressure and therefore occur as fragments and coatings as zones within the loess matrix, apart from recent voids. Thus, a pre-Holocene formation of a relic Bt horizon is probable. The main layer consists of loess mixed with pumice of the Laacher See eruption and shows clay accumulation in its basal part and impoverishment of clay in the upper part as a consequence of Holocene weathering and clay migration.

5.4 Burgkopf basalt quarry: autochthonous pre-Upper Oligocene Plinthosol

Near the village of Biebrich, the flat basalt dome, Burgkopf, rises above the Tertiary planation plain, covered by loessial periglacial layers with a strong admixture of Vallendar gravel, which intermits with the rise of the dome. The wall of a former quarry, in which basalt columns of the Upper Oligocene basalt duct were mined, exposes the profile of an autochthonous Plinthosol, about 4–6 m thick, above bleached saprolite from Devonian slates and sandstones (Table 17, Fig. 18). The volcanic basalt duct cuts through the paleosol which was preserved below a layer of laminated basalt tuff. This confirms a pre-Upper Oligocene age of the paleosol. High contents of clay above 50 mass % (Table 18) and pedogenic oxides (Table 19) indicate an intensive weathering

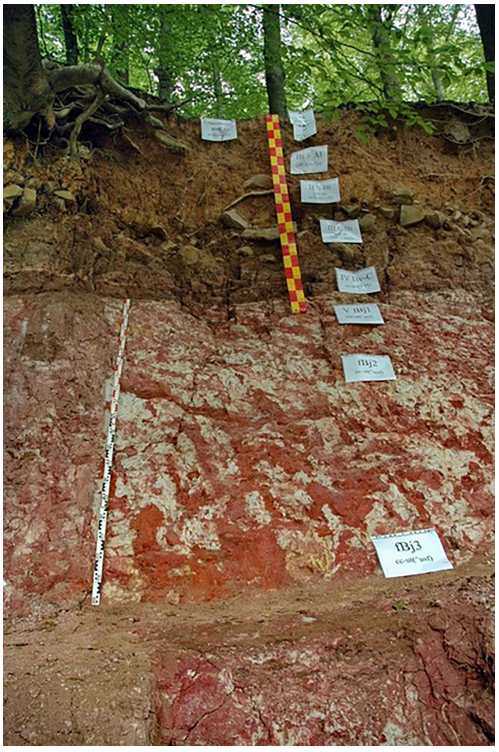

Figure 18. Burgkopf: pre-Upper Oligocene Plinthosol of the MTV, covered by a layer of Upper Oligocene basalt tuff and loessial periglacial layers.

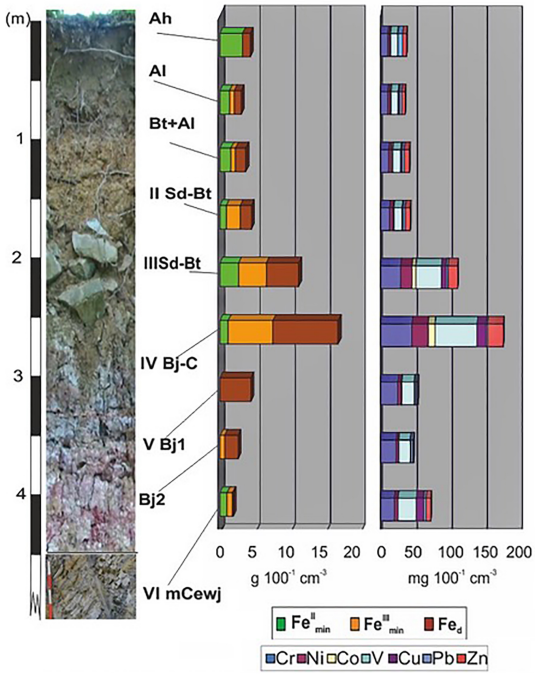

Figure 19. Burgkopf, pre-Upper Oligocene Plinthosol: volumetric masses of iron fractions (mineralogically bound Fe^{III}_{min} and Fe^{II}_{min}, as well as free iron oxides Fe_d) and trace elements of fresh slate and saprolite.

Table 17. Burgkopf: autochthonous pre-Upper Oligocene Plinthosol from saprolite, below Oligocene basalt tuff and Pleistocene periglacial layers of loess with fragments of basalt rock. Horizon symbols and characterization are according to AG Bodenkunde (2005). Depth refers to the lower boundary. Location: Burgkopf, near the village of Biebrich. TK 5613 Schaumburg r 3425088 h 5575723; 458 m a.s.l. Relief: near the crest of a basalt dome. WRB: (Stagnic) Luvisol.

Hor. no.	Horizon symbol	Depth (cm)	Horizon characteristics
1	Ah	6	Main layer of loess with pumice, dark yellow grey (5Y3/2) strong clayey silt (Ut4), weak to middle humic, fine crumbly, strongly rooted
2	Al	30	Main layer of loess with pumice, brownish yellow (10YR4/3) strong clayey silt (Ut4), weak humic spots, weakly rooted, sub-polyhedral to platy structure
3	Bt + Al	60	Main layer of loess with pumice, brownish yellow (10YR 4/3) and yellow brown zones (10YR 4/4), strong silty clay (Tu4, X1) with some horizontally orientated stones, weakly rooted, sub-polyhedral to polyhedral structure, dark brown zones with clay cutans, lower boundary interfingered with the horizon below
4	II S-Bt	100	Middle layer of loess and basalt, yellow brown (10YR 4/4) and dark brown (7.5YR5/4) zones, silty clay, moderate stony (Tu3, X2), weakly rooted, prism structure with dark brown clay cutans and spots of Mn oxides on ped surfaces, biopores with clay cutans, diffuse rusty mottles
5	III S-Bt	150	Basal layer of basalt tuff and some loess, yellowish brown (10YR 5/4) silty clay with basalt fragments and blocks (Tu3, Gr3, X3, mX), polyhedral to prismatic structure, weakly rooted, partly very strong compacted, diffuse rusty mottles, wavy lower boundary with accumulation of stones
6	IV Bv-C	190	Compact basalt tuff with alternating light grey, brown grey, red brown and purplish layers, centimetres thick, of clayey loam, strong gravelly and stony (Lt3, Gr4, X4), light olive grey inclusions of monomineralic smectite, coarse prismatic structure, sharp lower boundary marked by a concretionary band of goethite accumulation 1 cm thick
7	V fBj1	210	Paleogene Plinthosol, brown red (2.5YR 4/6) and purplish red (10R4/4) weak silty clay (Tu2) with white (10Y8/1) horizontally orientated spots, coarse prismatic to coherent structure, gliding transition
8	fBj2	300	Paleogene Plinthosol, red (10R4/4) silty clay (Tu3) with light grey to white (10Y8/1, 5BG8/1) spots, coherent to coarse prismatic structure, gliding transition
9	fBj3	400	Paleogene Plinthosol, purplish red (10R3/4) clayey loam (Lt3) with light grey (10Y8/1) and yellow red (5YR 6/6) spots, decreasing with depth, coherent to coarse prismatic structure, gliding transition
10	fBj4	500+	Paleogene Plinthosol, purplish red to red brown (10R6/3) silty loam (Lu) with a smaller part of light grey spots (5Y8/1), coherent to coarse prismatic structure

Table 18. Burgkopf: texture of the fine earth (< 2 mm), free of humus and carbonates. Fractions: c, m and f are coarse, middle and fine; S is sand, U is silt and T is clay. Depth refers to the lower boundary.

Horizon	Depth (cm)	Texture (mass %)						
		cS	mS	fS	cU	mU	fU	T
Ah	6	0.53	4.30	4.37	38.71	24.62	8.79	18.68
Al	30	0.39	4.04	4.44	42.05	21.66	9.14	18.28
Bt + Al	60	0.22	2.81	3.46	38.11	20.87	7.77	26.76
II S-Bt	100	0.19	4.19	4.67	32.80	18.31	7.86	31.99
III S-Bt	150	2.15	3.81	10.09	23.77	18.61	10.06	31.49
IV Bv-C	190	2.44	2.73	11.47	17.48	18.51	9.80	37.57
V fBj1	210	0.00	0.22	2.19	6.62	14.91	22.81	53.26
fBj2	300	0.10	0.36	11.47	20.94	15.37	15.17	36.59
fBj3	400	0.15	0.72	22.06	24.69	9.11	7.88	35.40
fBj4	500+	0.05	0.29	13.75	25.57	13.65	13.75	32.95

of the slate. The maximum of pedogenic iron, manganese and silica occurs in the uppermost horizon of the Plinthosol, which suggests a soil formation under the influence of a high groundwater table.

Besides illite, about 40–50 mass % of the clay fraction consist of kaolinite (Table 20). Weathering transformed all iron-bearing silicates completely to pedogenic iron oxides, and easy to mobilize heavy metals were leached (Fig. 19).

Table 19. Burgkopf: contents of pedogenic oxides. Depth refers to the lower boundary.

Horizon	Depth (cm)	Fe_o ($mg\,g^{-1}$)	Fe_d ($mg\,g^{-1}$)	Fe_o / Fe_d	Mn_d ($mg\,g^{-1}$)	Si_l ($mg\,g^{-1}$)	Al_l ($mg\,g^{-1}$)
Ah	6	2.80	9.10	0.31	0.14	4.18	7.62
Al	30	2.66	7.85	0.34	0.36	3.96	7.50
Bt + Al	60	2.58	10.33	0.25	0.39	4.42	8.85
II S-Bt	100	2.69	11.18	0.24	0.69	6.58	10.09
III S-Bt	150	1.50	30.54	0.05	0.64	9.01	12.41
IV Bv-C	190	1.11	61.62	0.02	1.69	13.32	16.71
V fBj1	210	0.12	39.45	0.00	0.09	10.33	9.84
fBj2	300	0.09	12.73	0.01	0.02	2.96	4.88
fBj3	400	0.08	15.29	0.01	0.02	3.06	5.82
fBj4	500+	0.06	8.02	0.01	0.01	3.62	5.59

Table 20. Burgkopf: clay mineral composition. LM is labile minerals > 1.8 nm, Sm is smectite, WL is mixed layer minerals, Chlp is primary chlorite, Chls is secondary (Al–)chlorite, Ver is vermiculite, Ill is illite, Kao icd is fireclay and Kao bad is *b*-axis disordered kaolinite; n.n. is not detectable. Depth refers to the lower boundary.

Horizon	Clay minerals < 2 µm (mass %)									
	Depth (cm)	Sm	WL	Chlp	Chls	Ver	WL	Ill	Kao icd	Kao bad
Ah	6	n.n.	9	n.n.	33	3	6	37	3	5
Al	30	n.n.	n.n.	n.n.	32	16	5	36	3	6
Bt + Al	60	n.n.	8	n.n.	32	3	13	39	2	3
II S-Bt	100	n.n.	8	n.n.	27	4	12	42	2	5
III S-Bt	150	9	12	n.n.	n.n.	n.n.	12	39	5	8
IV Bv-C	190	7	n.n.	n.n.	n.n.	n.n.	n.n.	0	73	20
V fBj1	210	n.n.	n.n.	n.n.	n.n.	n.n.	n.n.	57	21	22
fBj2	300	n.n.	n.n.	n.n.	n.n.	n.n.	n.n.	61	16	23
fBj3	400	n.n.	n.n.	n.n.	n.n.	n.n.	n.n.	57	24	19
fBj4	500+	n.n.	n.n.	n.n.	n.n.	n.n.	n.n.	56	19	24

* Masses calculated with reflex intensity × factor (Tributh and Lagaly, 1989).

The contents of pedogenic oxides are high and decrease with depth following the decreasing intensity of weathering.

During the eruption of the volcano, heat and moisture caused auto-hydrothermal processes that overprinted the layer of basalt tuff and led to silification and induration, as well as the formation of pure smectite concretions and veins. The basalt of the duct as well as a zone of the adjacent Plinthosol, 50 cm thick, also show a neo-formation of smectite.

Kaolinitization continued after the volcanic activity and caused the neo-formation of kaolinite from mafic minerals of the basalt tuff (Table 20).

The deposition of periglacial layers above the basalt tuff started with the accumulation of coarse fragments of basalt columns and boulders as a basal layer. The subsequently deposited loess of the middle layer invaded the hollows of the loosely packed rock fragments of the basal layer. The middle layer was subject to weathering and formation of a Luvisol during a pre-Holocene interglacial period. Micromorphological investigations of the Bt horizons show that clay cutans of former pores are disturbed and squeezed by frost pressure or cryoturbation, while recent pores show no signs of accumulation of fine clay. The main layer, which consists of a mixture of loess and pumice of the Late Pleistocene Laacher See eruption, shows a clear clay enrichment near the basis as a consequence of Holocene soil formation.

5.5 Wasenbach gravel pit: autochthonous Miocene Plinthosol

Several large gravel pits around the village of Wasenbach (Fig. 1) expose banks of pure, white quartz sand and gravel, several tens of metres thick, which stratigraphically belong to the youngest terrace (tT1 according to Requadt, 1990) of the Upper Oligocene Vallendar river system. In part, they derived from reworked gravel of an older terrace (tT2, after Requadt and Buhr, 1989) in a higher relief position. The sediments consist of alternating layers of quartz gravel, sand and kaolinitic sandy silt, deriving from the reworked weath-

Table 21. Wasenbach: autochthonous Miocene Plinthosol from Oligocene alluvial sediments above Vallendar gravel beds, covered by Pleistocene periglacial layers. Horizon symbols and characterization are according to AG Bodenkunde (2005). Depth refers to the lower boundary. Location: near the village of Wasenbach. TK25: 5613 Schaumburg r 3427002 h 5577275, 281 m a.s.l. Relief: gentle slope. WRB: Stagnic Luvisol.

Hor. no.	Horizon symbol	Depth (cm)	Horizon characteristics
1	Ah	17	Main layer of loess, grey-brown (10YR 3/4) strong clayey silt (Ut4), middle humic, middle rooted, low bulk density, crumb structure, sharp horizontal lower boundary
2	Sw-Al	35/60	Main layer of loess, yellowish brown (10YR 4/4) clayey silt (Ut3), weak humic, weakly rooted, low to middle bulk density, sub-polyhedral structure, gliding transition
3	II S-Bt	100	Middle layer of loess solifluction, dark yellow brown (10YR 5/6) silty clay, weak stony and gravelly (Tu3, X2, G2), near the basis alternating with solifluction layers with red brown (2.5YR 6/8) material from the lower horizon, coarse prismatic structure, sharp and wavy lower boundary
4	III C (fGroj) + Bt	140	Middle layer of loess solifluction, colour intensively changing between reddish brown (5YR 6/6), light brownish red (2.5YR 6/8) and brown (10YR 5/6), silty loam, gravelly (Lu3, G 3) coarse prismatic
5	IV C (fGroj)	180	Purplish red to red (10R 4/8) and yellow (2.5Y 8/6) layers of silty loam (Lu), platy structure, sharp lower boundary
6	V fGroj1	230	Miocene Plinthosol, purplish red to red (10R 4/4 to 10R 4/8) silty loam (Lu) with yellow spots (2.5Y 8/6), horizontally orientated in the uppermost decimetre
7	fGroj2	350	Miocene Plinthosol, large yellow (2.5Y 8/6) spots of strong clayey silt (Ut4) alternating with purplish red spots (10R 4/8) of silty fine sand (fSu3), sharp lower boundary
8	VI fGorj	450	Orange-brown (10YR 8/6-6/6) silty middle sand (mSu3)
9	fGrj	1000+	Upper Oligocene Vallendar gravel, grey-white (N 8/0) silty middle sand and banks of gravel (mSu3, G), with banks of ferruginous silcrete centimetres to decimetres thick

Table 22. Wasenbach: texture of the fine earth (< 2 mm), free of humus and carbonates. Fractions: c, m and f are coarse, middle and fine; S is sand, U is silt, T is clay, y is yellow and r is red. Depth refers to the lower boundary.

Horizon	Depth (cm)	Texture (mass %)						
		cS	mS	fS	cU	mU	fU	T
Ah	17	0.67	7.17	8.45	34.93	22.83	8.31	17.62
Sw-Al	35/60	0.78	7.51	7.42	36.99	22.27	8.60	16.43
IIS-Bt	100	2.69	4.54	6.77	30.43	18.20	6.89	30.48
IIIC(fGroj) + Bt	140	2.06	4.68	11.38	23.89	16.09	12.23	29.67
IVC(fGroj)	180	0.13	0.54	9.49	27.40	20.27	15.10	27.06
VfGroj1(y)	230	0.83	5.51	19.97	28.58	14.90	10.42	19.79
VfGroj1(r)	230	0.60	5.31	20.89	26.98	14.93	10.94	20.35
fGroj2(y)	350	0.71	12.07	36.46	22.18	8.43	6.48	13.67
fGroj2(r)	350	2.23	25.85	45.13	10.87	4.91	4.11	6.91
VIfGorj	450	0.11	16.53	53.11	13.35	4.58	3.97	8.35
fGrj	1000+	32.35	33.47	21.40	5.16	1.42	2.23	3.96

Table 23. Wasenbach: contents of pedogenic oxides; y is yellow and r is red. Depth refers to the lower boundary.

Horizon	Depth (cm)	Fe_o (mg g^{-1})	Fe_d (mg g^{-1})	Fe_o / Fe_d	Mn_d (mg g^{-1})	Si_l (mg g^{-1})	Al_l (mg g^{-1})
Ah	17	3.17	6.99	0.45	0.94	10.92	6.76
Sw-Al	35/60	3.33	7.41	0.45	0.95	12.25	7.71
IIS-Bt	100	1.27	13.35	0.10	0.18	12.81	9.21
IIIC(fGroj) + Bt	140	0.09	22.22	0.00	0.07	8.66	5.62
IVC(fGroj)	180	0.07	24.25	0.00	0.05	7.97	6.14
VfGroj1(y)	230	0.05	31.81	0.00	0.03	6.92	5.16
VfGroj1(r)	230	0.36	32.11	0.01	0.03	7.50	5.67
fGroj2(y)	350	0.04	3.56	0.01	0.01	5.73	4.24
fGroj2(r)	350	0.06	11.33	0.01	0.02	4.51	3.64
VIfGorj	450	0.04	5.21	0.01	0.02	5.73	4.24
fGrj	1000+	0.03	0.08	0.33	0.01	4.75	3.64

Table 24. Wasenbach: clay mineral composition. LM is labile minerals > 1.8 nm, Sm is smectite, WL is mixed layer minerals, Chlp is primary chlorite, Chls is secondary (Al–)chlorite, Ver is vermiculite, Ill is illite, Kao icd is fireclay and Kao bad is *b*-axis disordered kaolinite; n.n. refers to values that are not detectable.

Horizon	Depth (cm)	Clay minerals < 2 µm (mass %)									
		LM	Sm	WL	Chlp	Chls	Ver	WL	Ill	Kao icd	Kao bad
Ah	17	3	0	0	0	0	0	16	72	6	3
Sw-Al	35/60	4	0	2	0	21	0	12	49	8	4
IIS-Bt	100	0	8	6	0	0	0	6	41	23	15
IIIC(fGroj) + Bt	140	0	0	0	0	0	0	0	56	30	14
IVC(fGroj)	180	0	0	0	0	0	0	0	56	30	14
VfGroj1(y)	230	0	0	0	0	0	0	0	55	34	11
VfGroj1(r)	230	0	0	0	0	0	0	0	57	33	10
fGroj2(y)	350	0	0	0	0	0	0	0	53	35	12
fGroj2(r)	350	0	0	0	0	0	0	0	56	35	9
VIfGorj	450	0	0	0	0	0	0	0	55	33	13
fGrj	1000+	0	0	0	0	0	0	0	49	32	20

* Masses calculated with reflex intensity × factor (Tributh and Lagaly, 1989); y is yellow and r is red. Depth refers to the lower boundary.

ering mantle. The abrupt changes in particle size, intercalated channel structures and banks of ferrous silcrete indicate the activity of a shallow river with intermittent rates of streamflow. Such sediments are typical of semi-arid climatic conditions with alternating rain and dry seasons. The fluvial sediments change from gravel to sand up to the surface and the contents of fine material progressively increases. The uppermost layer was deposited as flood plain sediments, rich in silt and clay, from which an autochthonous Plinthosol with intensive red, white and yellow mottles developed under the influence of an intermittent depth of the groundwater table (Fig. 20, Table 21). Soil development occurred probably during the Miocene. The contents of silt and clay (Table 22) and pedogenic oxides (Table 23), as well as total amounts of Al, Fe and heavy metals, bound in silicates, increase from the lowermost horizon to the surface of the Plinthosol. The clay fraction consists of illite and kaolinite in similar proportions (∼ 40 % kaolinite and ∼ 60 % illite) in all horizons (Table 24). Kaolinites of the Vallendar gravel mainly derive from reworked saprolite. The proportion of kaolinite increases from the gravel to the upper Plinthosol horizons and indicates that erosion of terrestrial kaolinitic soils (e.g. Ferralsols, Plinthosols) may have delivered the fines of the flood plain sediment rather than the weathering of primary silicates in situ.

With increasing inclination of the land surface in the direction of the former Tertiary trough valley the paleosol during Pleistocene cold phases was affected by soil creep and slope downwards, increasingly incorporated into basal solifluction layers. The basal layer of the periglacial slope deposits consists of horizontally laminated, redistributed Plinthosol material. The middle layer, rich in loess with quartz gravel, and the main layer, consisting of a mixture of loess with Laacher See pumice, superimpose the basal layer. Both layers served as parent material for the Holocene Stagnic Luvisol.

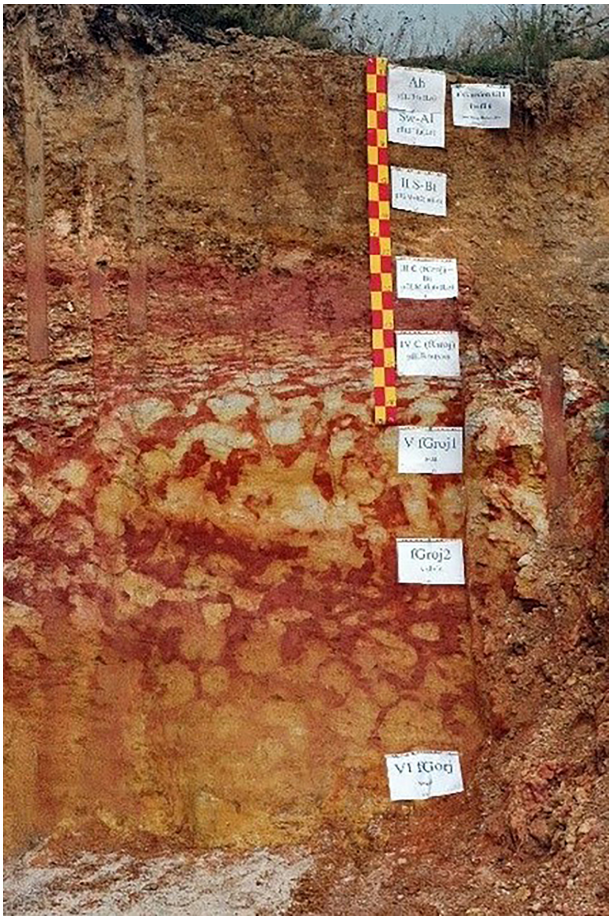

Figure 20. Wasenbach: Miocene Plinthosol from alluvial flood plain sediments above Upper Oligocene Vallendar gravel, covered by loessial periglacial layers.

Data availability. All underlying data are published in the figures and tables of this article. There are no external data.

Competing interests. The author declares that there is no conflict of interest.

Acknowledgements. Werner Heuser of the Stephan Schmidt KG, Dornburg/Langendernbach, as well as Arndt Nikolaus Loh of the Theodor Stephan KG GmbH & Co.KG in Burbach-Niederdresselndorf, supported the access to the excursion sites in Eisenbach as well as preparation of the profiles. I am grateful for the active help of Einar Eberhardt and Vincent J. N. M. L. Felde in the field and many fruitful discussions.

References

AG Bodenkunde: Bodenkundliche Kartieranleitung, 5th Edn., 438 pp., Schweizerbart, Stuttgart, 2005.

Ahlburg, J.: Über das Tertiär und das Diluvium im Flußgebiete der Lahn, Jahrbuch der preußischen Geologischen Landesanstalt, 36, 269–379, 1915.

Andres, W., Bibus, E., and Semmel, A.: Tertiäre Formenelemente in der Idsteiner Senke und im Eppsteiner Horst (Taunus), Z. Geomorphol., 18, 339–349, 1974.

Blume, H.-P., Stahr, K., and Leinweber, P.: Bodenkundliches Praktikum, 3rd Edn., Spektrum, Heidelberg, 2011 (in German).

Brindley, G. W. and Gillery, F. H.: X-ray identification of chlorite species, Am. Mineral., 41, 169–186, 1956.

Felix-Henningsen, P.: Die mesozoisch-tertiäre Verwitterungsdecke (MTV) im Rheinischen Schiefergebirge – Aufbau, Genese und quartäre Überprägung, Relief, Boden, Paläoklima, 6, 192 pp., Borntraeger, Berlin-Stuttgart, 1990.

Felix-Henningsen, P.: Mesozoic Tertiary weathering and soil formation on slates of the Rhenish Massif (Germany), Catena, 21, 229–242, 1994.

Felix-Henningsen, P.: Saprolite, in: Handbuch der Bodenkunde, edited by: Blume, H.-P., Felix-Henningsen, P., Frede, H.-G., Guggenberger, G., Horn, R., and Stahr, K., 40th Edn., 01/15, chap. 2.1.5.2, 1–34, Wiley – VCH, Stuttgart, 2015.

Felix-Henningsen, P. and Requadt, H.: Mineralogische und geochemische Untersuchungen der mesozoisch-tertiären Verwitterungsdecke im Gebiet der südwestlichen Lahnmulde (Rheinisches Schiefergebirge), Geologisches Jahrbuch Hessen, 113, 217–228, 1985.

Felix-Henningsen, P. and Wiechmann, H.: Ein mächtiges autochthones Bodenprofil präoligozänen Alters aus unterdevonischen Schiefern der nordöstlichen Eifel, Z. Pflanz. Bodenkunde, 148, 147–158, 1985.

Felix-Henningsen, P., Spies, E.-D., and Zakosek, H.: Genese und Stratigraphie periglazialer Deckschichten auf der Hochfläche des Ost-Hunsrücks (Rheinisches Schiefergebirge), Eiszeitalter u. Gegenwart, 41, 56–69, 1991.

Islam, A. K. M. E. and Lotse, E. G.: Quantitative mineralogical analysis of some Bangladesh soils with x-ray, ion exchange and selective dissolution techniques, Clay Miner., 21, 31–42, 1986.

Löhnertz, W.: Zur Altersstellung der tiefliegenden fluviatilen Tertiärablagerungen der SE-Eifel, Neues Jahrbuch für Geologie und Paläontologie, Abhandlungen, 166, 179–206, 1978.

Makumbi, M. N. and Herbillon, A. J.: Weathering of chlorite in a soil derived from a chloritoshist under humid tropical conditions, Geoderma, 13, 89–104, 1975.

Mosebach, R.: Zur petrographischen Kenntnis devonischer Dachschiefer, Notizblatt des Hessischen Landesmtes für Bodenforschung, 82, 234–246, Wiesbaden, 1954.

Müller, K.-H.: Morphologie des zentralen Hintertaunus und des Limburger Beckens. Ein Beitrag zur tertiären Formengenese, PhD, Univ. Marburg. Marburger Geographische Schriften, 112 pp., 1973.

Requadt, H.: Erläuterungen Blatt 5613 Schaumburg, Geologische Karte von Rheinland-Pfalz 1 : 25 000, 2nd Edn., Geologisches Landesamt Rheinland-Pfalz, Mainz, 1990.

Requadt, H. and Buhr, R.: Gliederung und Paläogeographie der tertiären "Vallendarer Schotter" im Hintertaunus, Zeitschrift der Deutschen Geologischen Gesellschaft, 140, 333–342, 1989.

Sauer, D. and Felix-Henningsen, P.: Saprolite, soils, and sediments in the Rhenish Massif as records of climate and landscape history, Quaternary Int., 156–157, 4–12, 2006.

Semmel, A.: Reliefentwicklung im Rheinischen Schiefergebirge-neue Befunde, neue Probleme: Zur präquartären Entwicklung, 44. Deutscher Geographentag Münster, 24. bis 28. Mai 1983, Tagungsbericht und wissenschaftliche Abhandlungen, Stuttgart, 71–74, 1984.

Spies, E.-D.: Vergleichende Untersuchungen an präpleistozänen Verwitterungsdecken im Osthunsrück und an Gesteinszersatz durch ascendente (Thermal-) Wässer in der Nordosteifel (Rheinisches Schiefergebirge), 182 pp., PhD, Bonn, 1986.

Till, R. and Spears, D. A.: The determination of quartz in sedimentary rocks using X-ray diffraction method, Clay. Clay Miner., 17, 323–327, 1969.

Tributh, H. and Lagaly, G.: Identifizierung und Charakterisierung von Tonmineralen, Berichte der Deutschen Ton- und Tonmineralgruppe e.V., Giessen, 1–162, 1989.

Walter, R.: Geologie von Mitteleuropa, 6th Edn., Schweizerbart, Stuttgart, 1995.

Weaver, C. E. and Pollard, L. D.: The chemistry of clay minerals, Developments in Sedimentology, 15, 213 pp., Elsevier, Amsterdam, London, 1973.